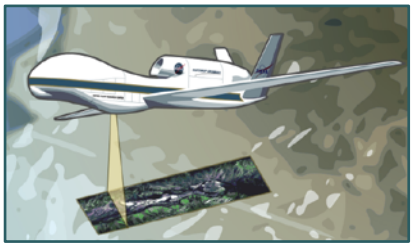

UAVSAR Processing and Examples

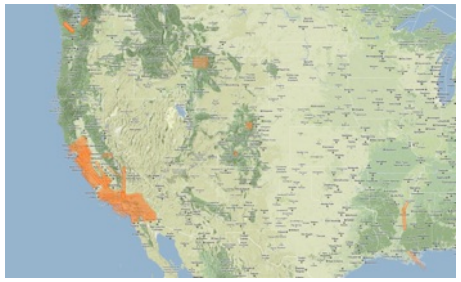

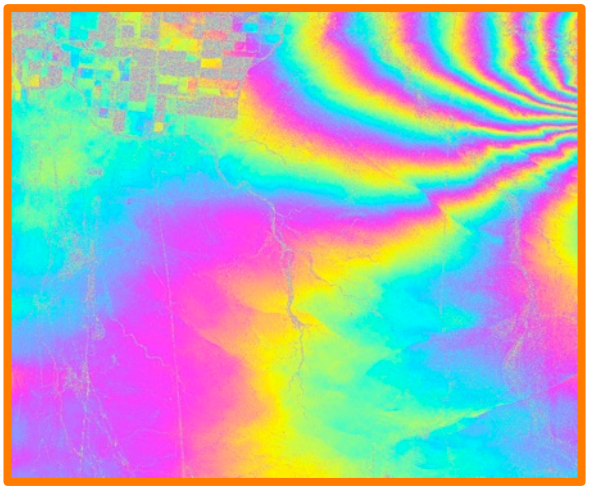

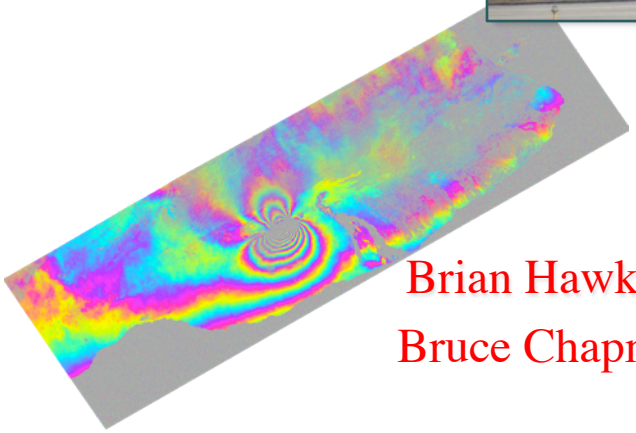

by

Scott Hensley, Thierry Michel, Ron Muellerschoen,
Brian Hawkins, Cathleen Jones, Maxim Neumann, Marco Lavalle, Alex Fore,
Bruce Chapman, Razi Ahmed, Yang Zheng, Joanne Shimada and Yunling Lou

Jet Propulsion Laboratory, California Institute of Technology

March 26, 2013

Processing

UAVSAR End-to-End Flow

UAVSAR end-to-end operation involves multiple organizations

Submit flight request at Ames' online SOFRS

ARC
Airborne Science Program
Science Operations Flight Request System (SOFRS)

Plan flight lines using JPL's online Flight Planning System

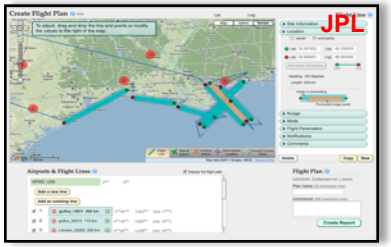

ESD Program Manager

Approve flight request

Principal Investigator

Archive processed data at ASF

Processed data are available through JPL's UAVSAR Data Search portal and ASF's SAR Data Center portal

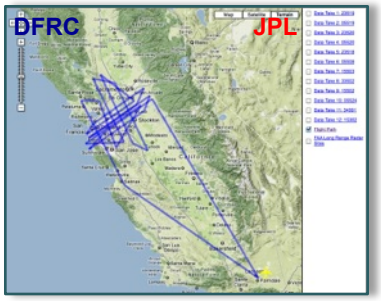

Develop flight plan and schedule flight

Execute flight plan to acquire data

Download radar data to Ground Data System for processing

Perform SAR processing at Ames' Columbia supercomputing facility

Strip Mode Processing

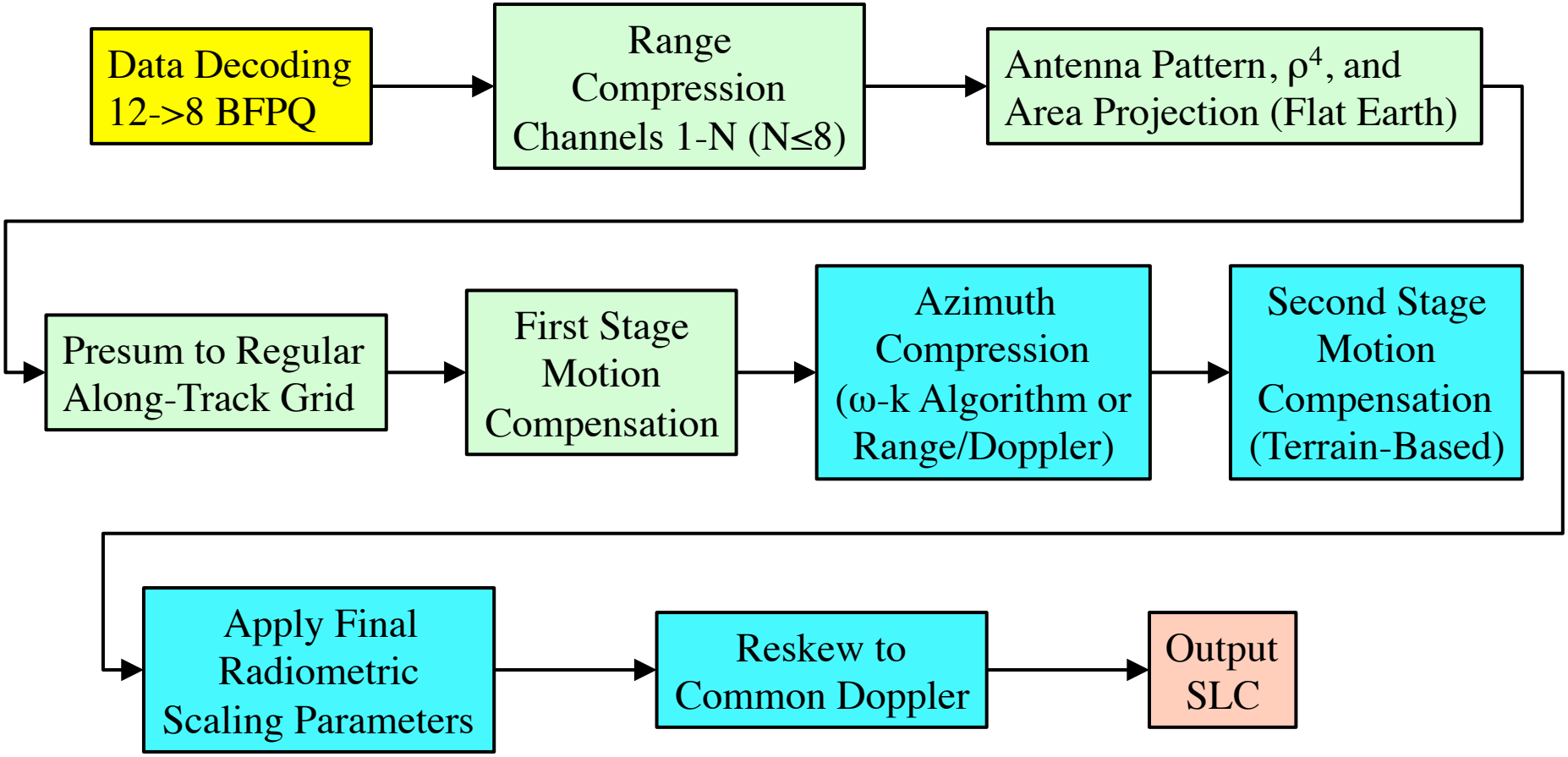

RTI Processing

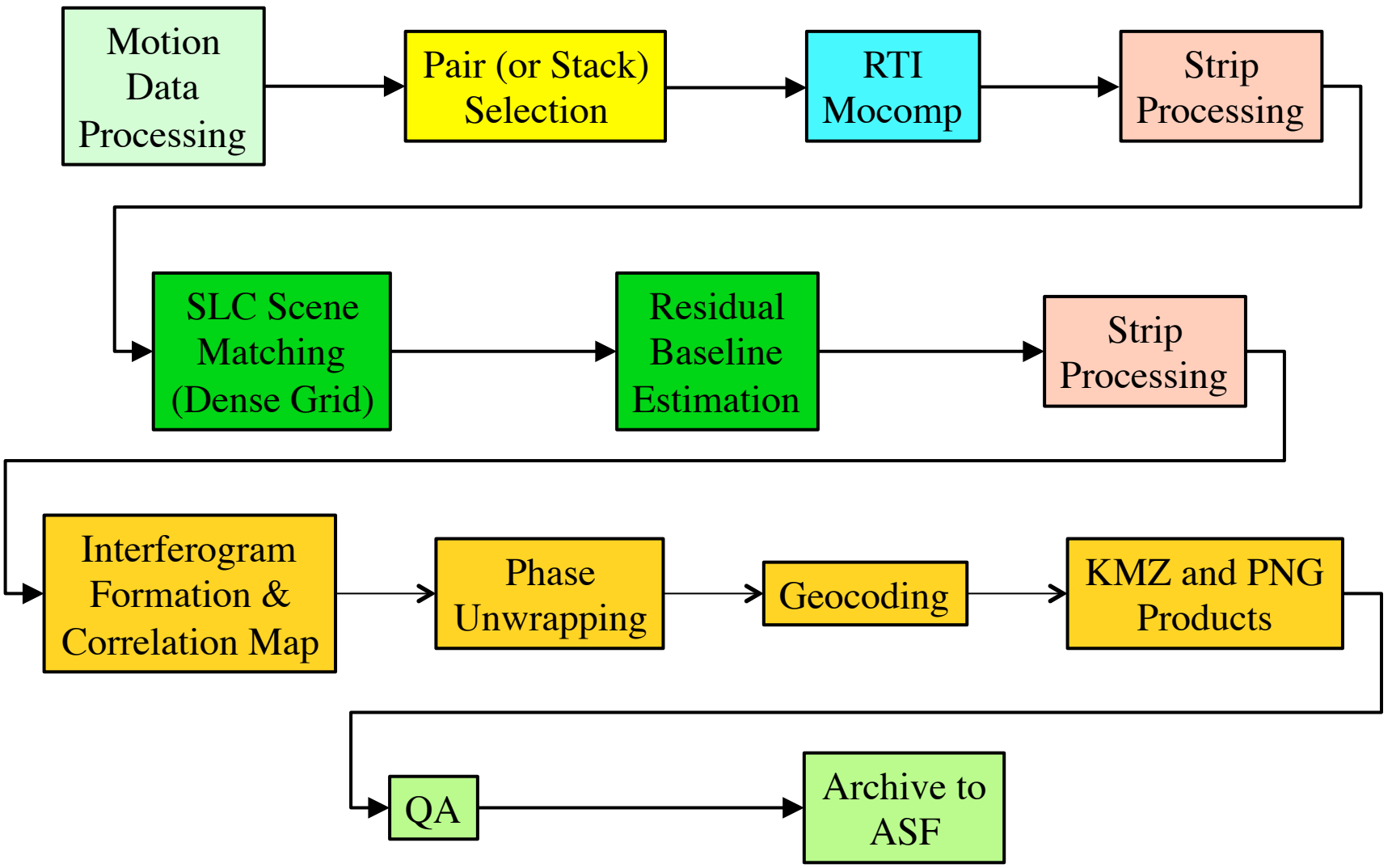

JPL

Processing Challenges

Processing Challenges

- Processing challenges for UAVSAR L-band data fall into three major categories:
  - **Residual Motion Estimation:** Estimating sub-centimeter relative motion between repeat pass flight lines.
  - **Throughput:** Generating sufficient numbers of repeat pass interferograms to meet investigator needs.
  - **Algorithmic Issues:** Identifying and correcting/refining errors and/or non-optimal algorithms used to process the data.
- Work is being conducted in all three areas to support both geodetic and forest mapping applications.
  - New algorithm being implemented that will work even when there is a large deformation signature in the scene.
  - Working on implementing a stack processing option that changes the quadratic problem back to a linear problem.
  - Identifying and fixing algorithmic bugs related to long baseline and high squint processing. We have determined these problems are related.

Spaceborne versus Airborne Radar Geodesy - I

- Both spaceborne and airborne radar systems can play a role in geodetic measurements, however, there are notable differences between these types of systems that impact measurement applicability.

Comparison Point	Spaceborne	Airborne
Imaging Geometry	Limited by the law of orbital mechanics. North/South deformation signal typically not as well resolved as vertical or east/west signals.	Imaging geometry can be chosen to optimize observation scenario.
Revisit Time	Typical orbital repeat intervals are from 10-45 days. Quicker revisit times typically require SAR constellations.	Revisit time can be tailored to meet geophysical application ranging from minutes to years.
Mapping Scale	Supports mapping deformation from local to global scales.	Ideally suited to regional mapping applications. Size of region dictated by platform type and cost of logistics and operations.
Accessibility	Global accessibility.	Limited by platform type and ability to obtain access to airspace.

Spaceborne versus Airborne Radar Geodesy-II

Comparison Point	Spaceborne	Airborne
Baseline Estimation	Precision orbit data often accurate enough for deformation signal determination. Residual baseline estimation when required involves simple linear or quadratic models.	Motion metrology for airborne platforms, combined INU/GPS, not sufficiently accurate to support geodetic observations. Residual baselines have high spatial frequency components. Residual baseline estimation is data driven and requires appropriate observations well distributed in both range and along-track.
Atmosphere	Tropospheric changes between observations affects phase.	Most tropospheric changes affecting phase measurements occur in several kilometers above ground, therefore magnitude similar to spaceborne case.
Ionosphere	Ionospheric distortion to phase measurements, problem is worse for longer wavelengths.	No ionospheric distortion.

- Other sensor choices also have a major impact on geodetic imaging performance, e.g., wavelength (affects temporal correlation), SNR (measurement precision), etc…

JPL

Residual Motion Estimation

Measured Offsets for Central Valley

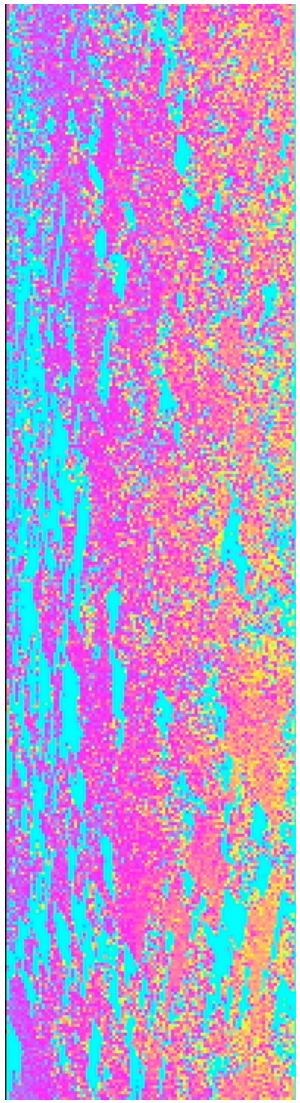

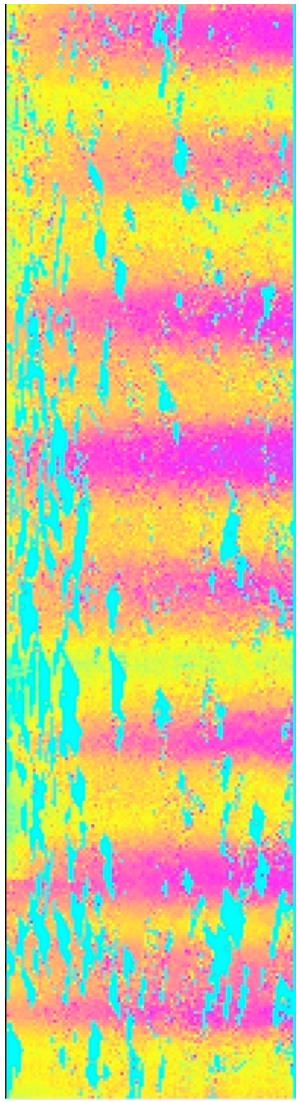

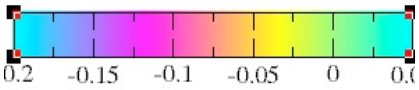

Range offset, Δρ (pix)
1.66 m /pix

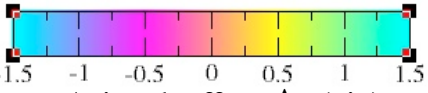

Azimuth offset, Δs (pix)
0.6 m /pix

- Residual motion estimation currently uses offset or image displacement measurements between the two images comprising the interferometric pair to estimate the residual motion.
- The electronically scanned antenna complicates the formulas for residual motion estimation compared with flush mounted antennas used by most airborne systems.

$$\Delta\rho = \langle \Delta\vec{b}, \hat{\ell} \rangle$$

$$\Delta s = \left[\frac{\sin\alpha\langle \vec{b}, \hat{\ell} \rangle - \langle \vec{b}, M\hat{n} \rangle + \rho\hat{\ell}_c \frac{\partial b_c}{\partial s} + \rho\hat{\ell}_h \frac{\partial b_h}{\partial s}}{\langle \hat{v}, \hat{n} \rangle - \sin\alpha\langle \hat{v}, \hat{\ell} \rangle} \right] \langle \hat{v}, \hat{s} \rangle$$

Residual Motion Removed

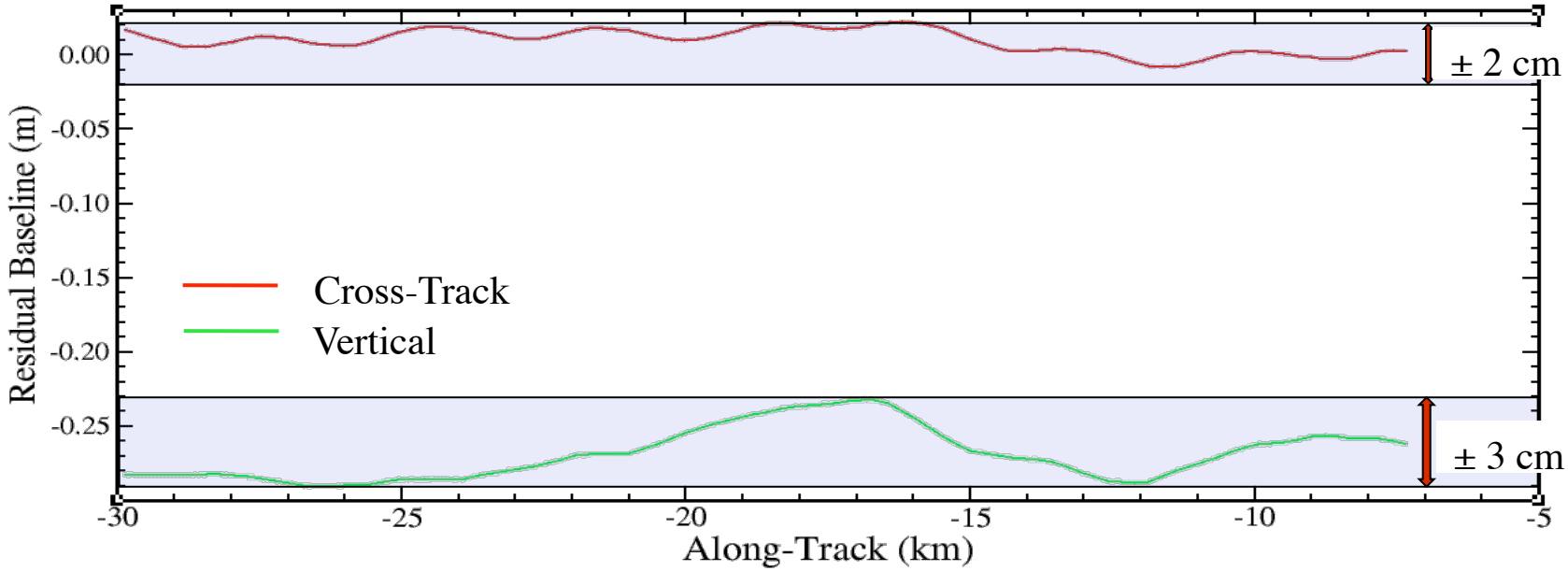

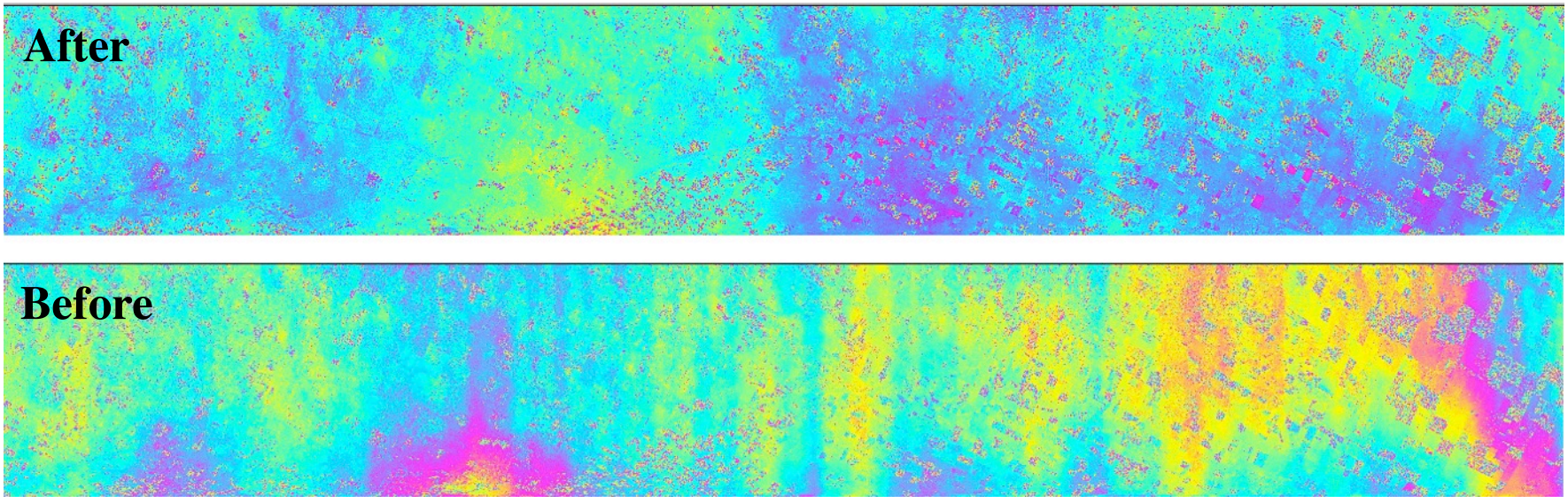

Avoid Residual Motion Compensation?

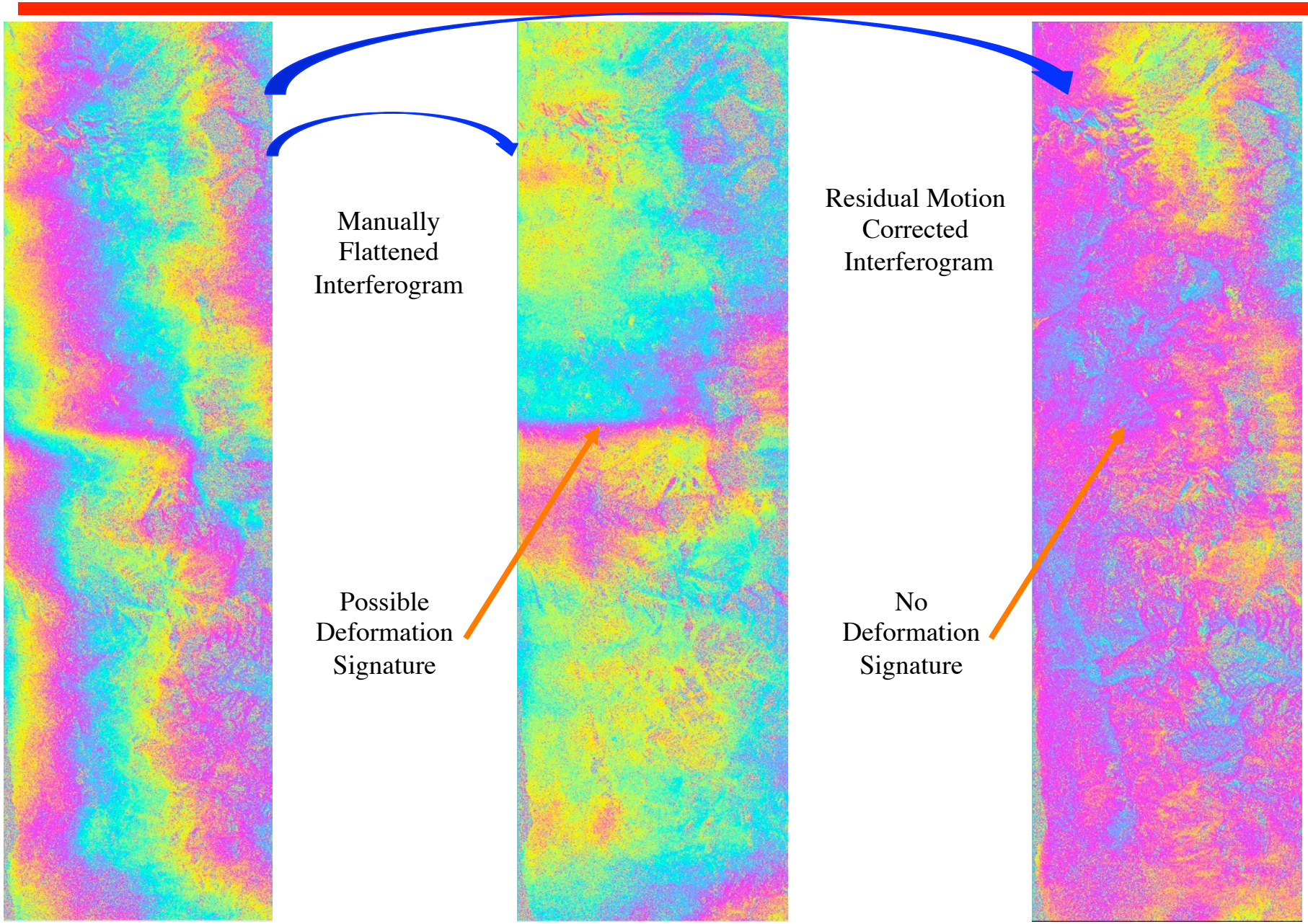

JPL

Throughput Challenges

A Combinatorial Challenge…

- The combinatorial nature of interferometric processing.

N_L = Number of Interferometric Flight Lines Flown

M_j = Number of Lines Flown for the j^{th} Flight Line

$$M_j = \sum_{i=1}^{Y_j} m_{ij}$$ where m_{ij} is the number of lines flown in the i^{th} year for the j^{th} flight line and Y_j is the number of years flown

$$T_p = \sum_{j=1}^{N_L} \frac{M_j(M_j-1)}{2} = \sum_{j=1}^{N_L} \frac{\left(\sum_{i=1}^{Y_j} m_{ij}\right)\left(\left(\sum_{i=1}^{Y_j} m_{ij}\right)-1\right)}{2}$$

$$M = \frac{7(7-1)}{2} = 21$$

	1	2	3	4	5	6	7
1		1	2	3	4	5	6
2			7	8	9	10	11
3				12	13	14	15
4					16	17	18
5						19	20
6							21
7							

Interferometric Processing – Stack Option

- Total interferometric pairs is linear with the number of interferometric lines flown but is quadratic in the number of lines flown for that line.
- Because residual motion estimation is pairwise dependent the compute resources are insufficient to process every pair (setting aside the ability to examine all the pairs).
- Several possibilities:
  - Limit investigators processing to some function that is linear in the number of lines flown for each repeat pass line.
    - Additional logistical issues when flight lines are split over multiple years.
  - **Change processing paradigm:**
    - Working on stack processing where groups of lines are processed together.
      - Advantages: Allows making interferometric observations for all passes in the stack.
      - Disadvantages: Can not achieve optimal interferometric performance for all pairs in the stack.

JPL

Correlation Anomalies

Correlation Anomalies

- In the stack processing of long baseline data for forest structure applications we noted that the magnitude of the observed correlation for short temporal baselines seemed to be smaller than expected.
  - Generated a tool to predict the SNR correlation based on image backscatter and measured scene offsets.
  - Using these tools identified two issues.

Actual Correlation

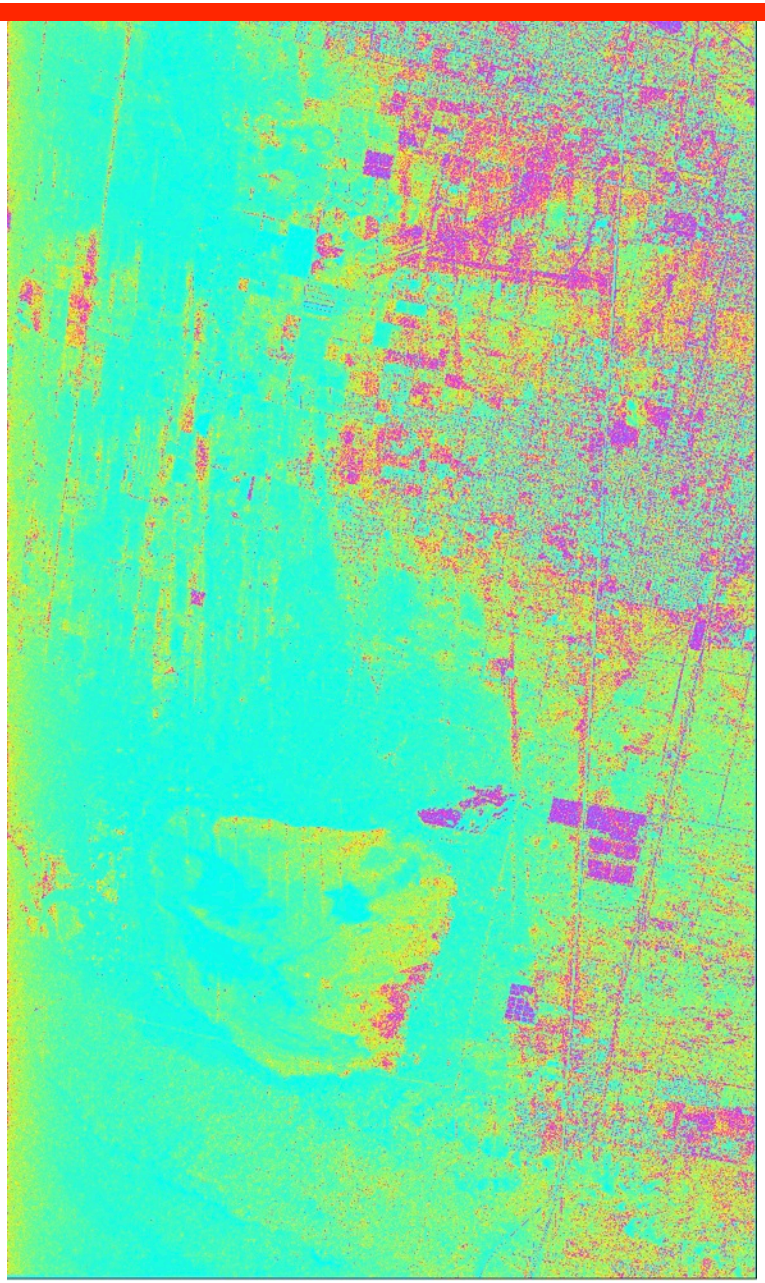

Rosamond Data
From 2011
$\Delta t < 1hr$

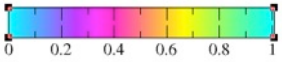

Simulated Correlation – 8 dB Bias

Actual Correlation

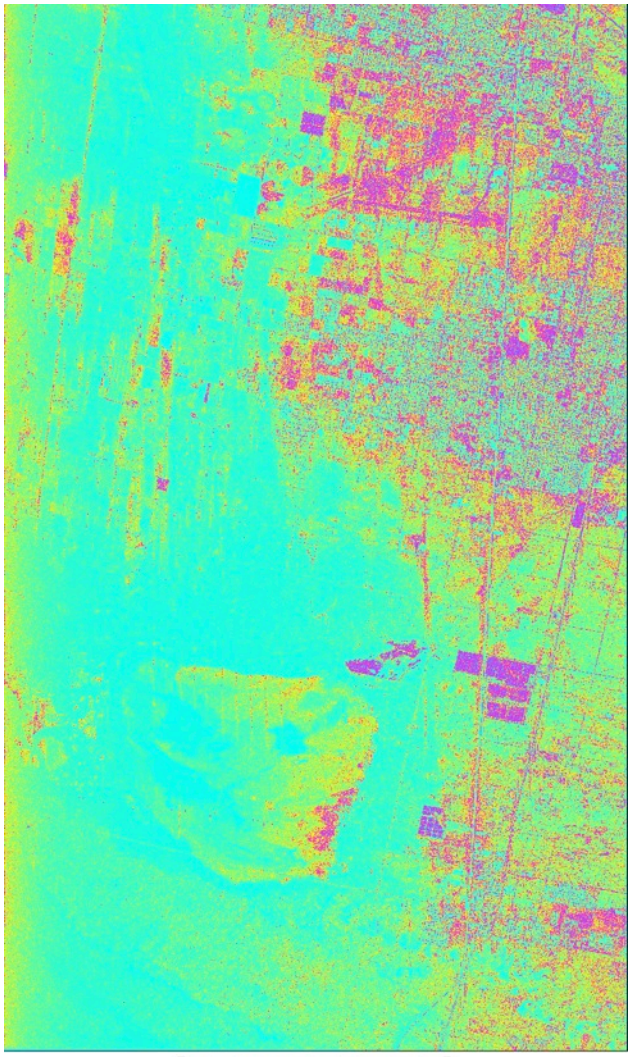

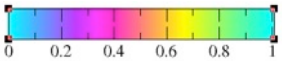

Correlation

Simulated Correlation

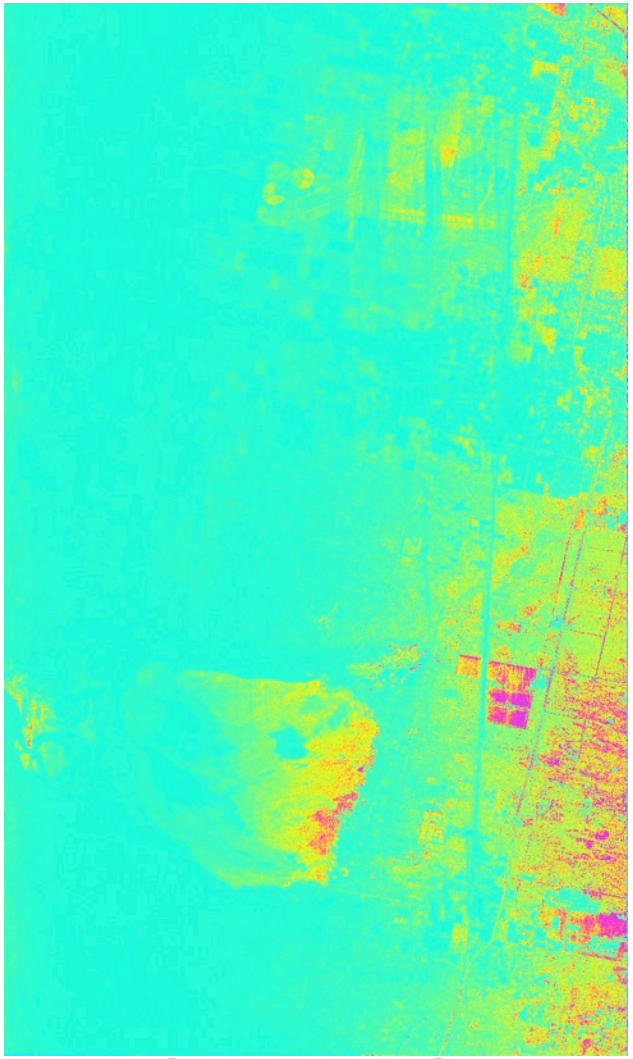

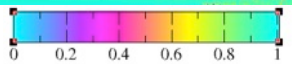

Correlation

Correlation Ratio

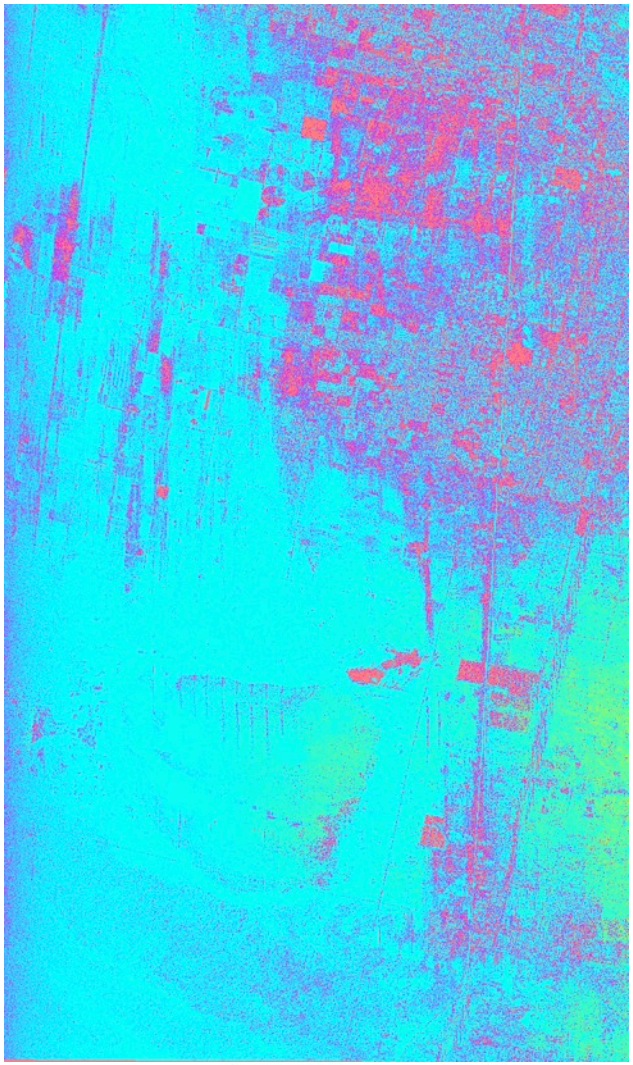

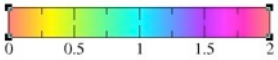

Correlation Ratio

SNR Discrepancy…

- We have partially resolved the SNT discrepancy. Using the sniffer pulse data we shown that the effective noise equivalent so is is scene dependent which we think is due to background RFI. Work continue to fully quantify.

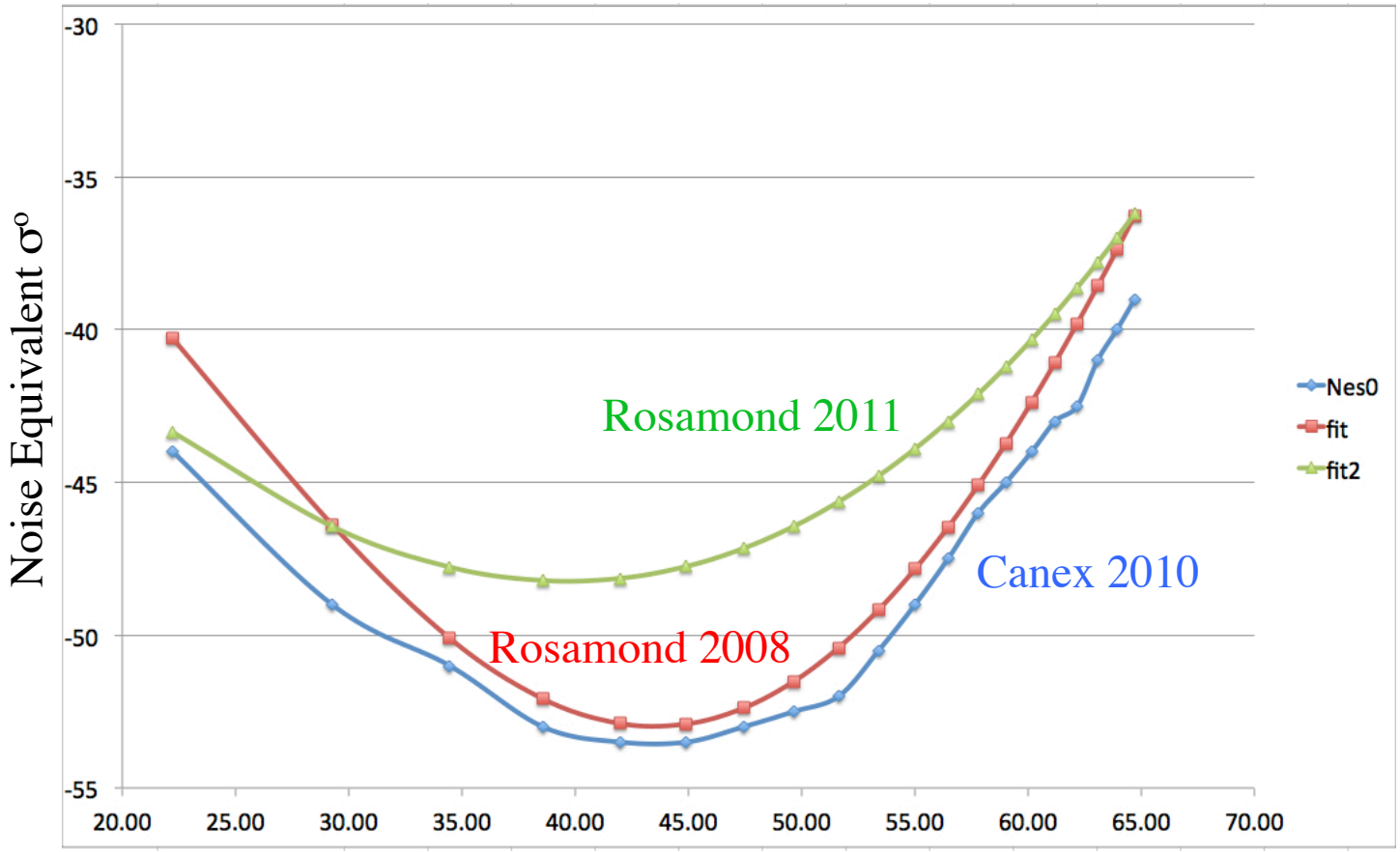

Towards a Solution…

Actual Correlation

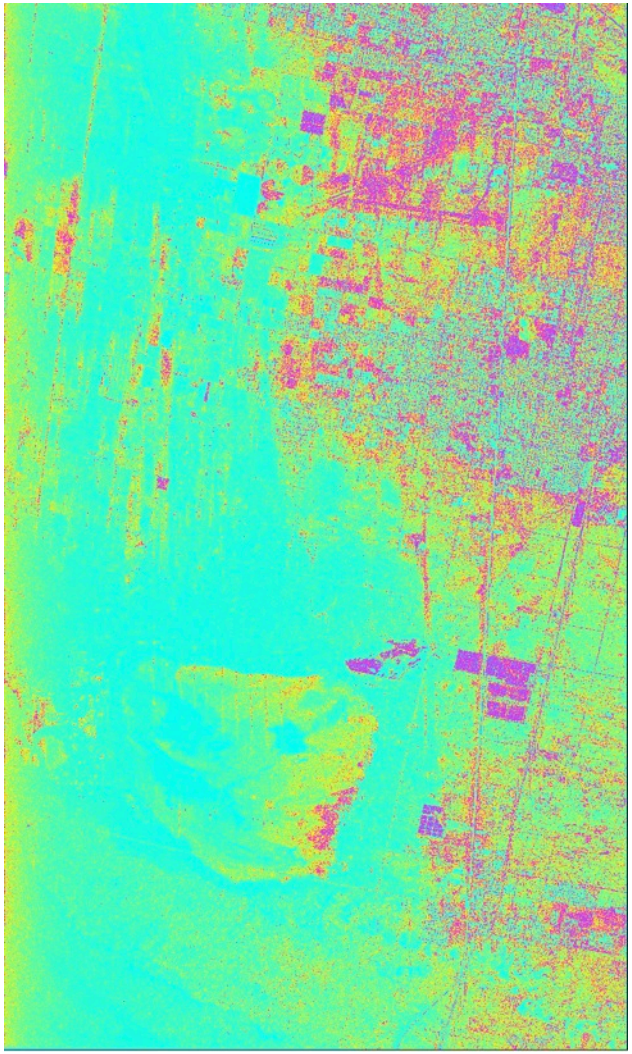

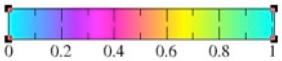

Correlation

Simulated Correlation

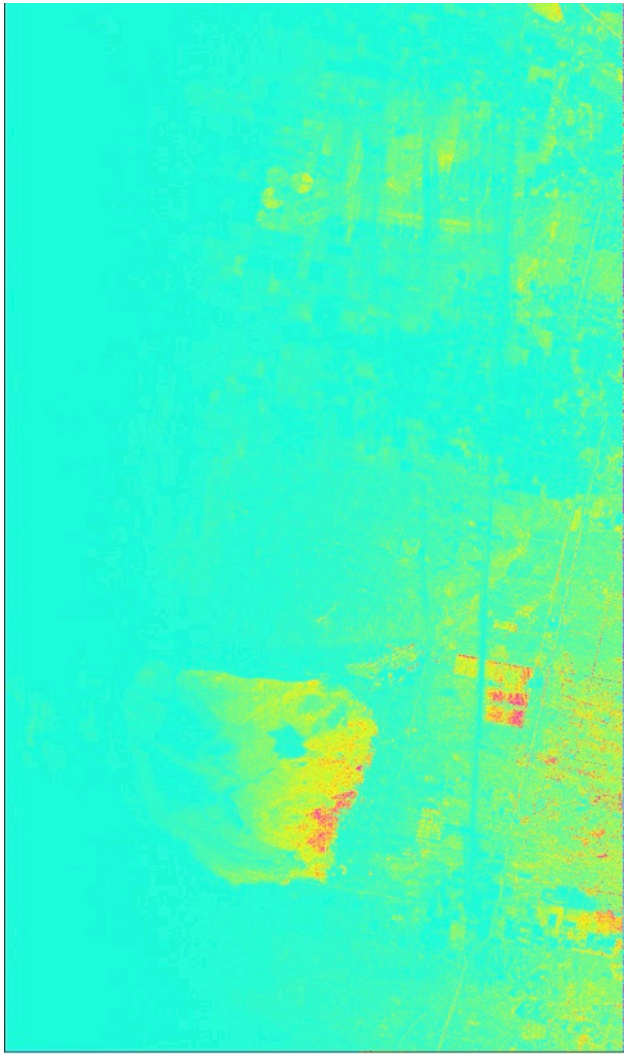

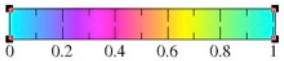

Correlation

SNR Bias

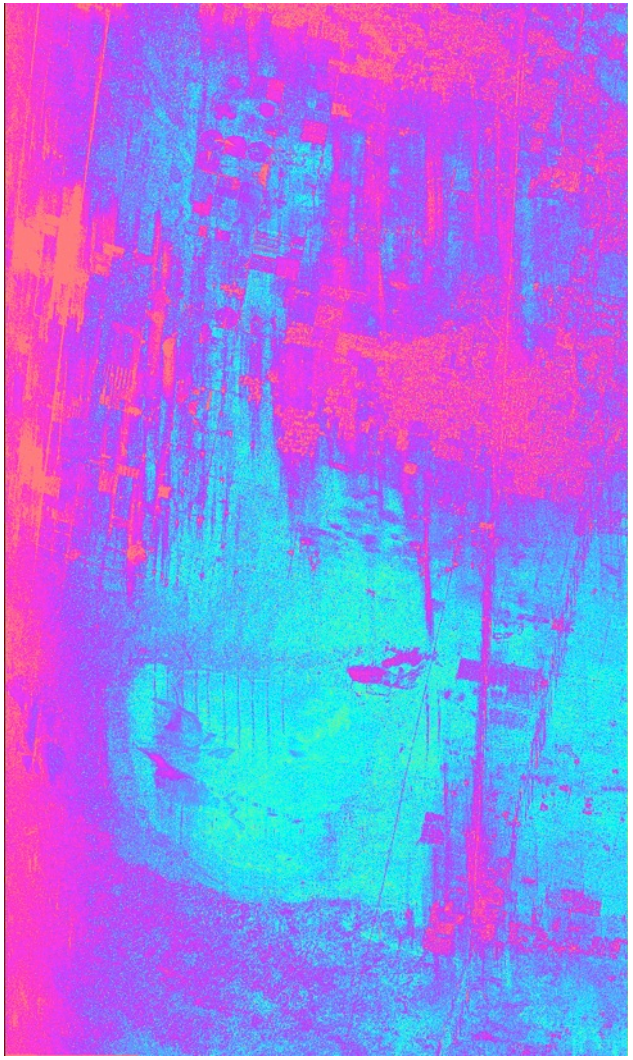

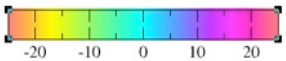

SNR Bias

Baseline Dependent Correlation

- For a flat area in Harvard forest observed correlation in area where should be constant decreased with baseline length. Several possible explanation were investigated.

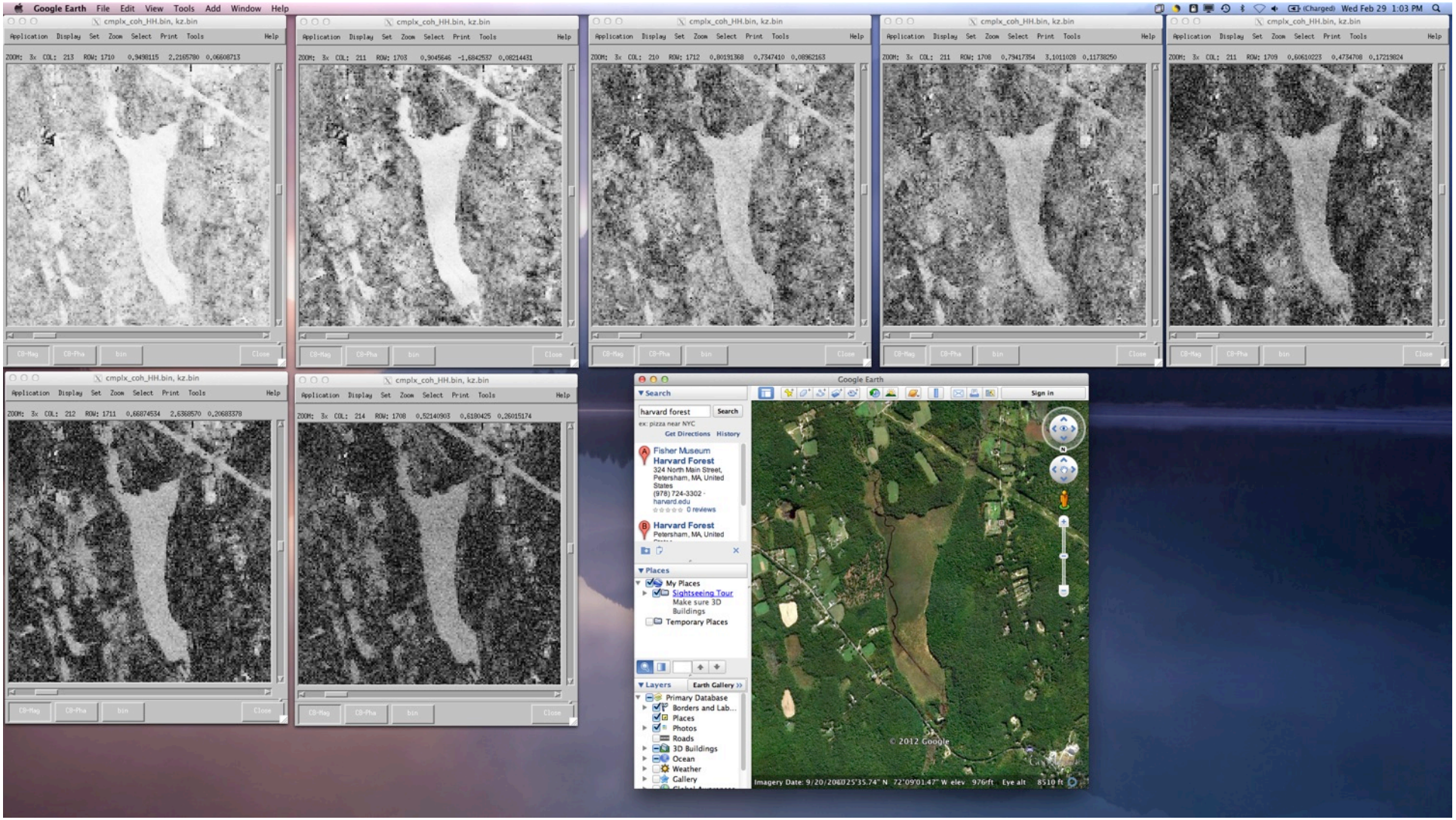

Root Cause Detected

- Reduced correlation is partially a result of image offsets between the image pairs that is a function of baseline length.
  - Problem is a mHz Doppler processing that we have isolated to two subroutines.
  - Similar issue with large squint angles.

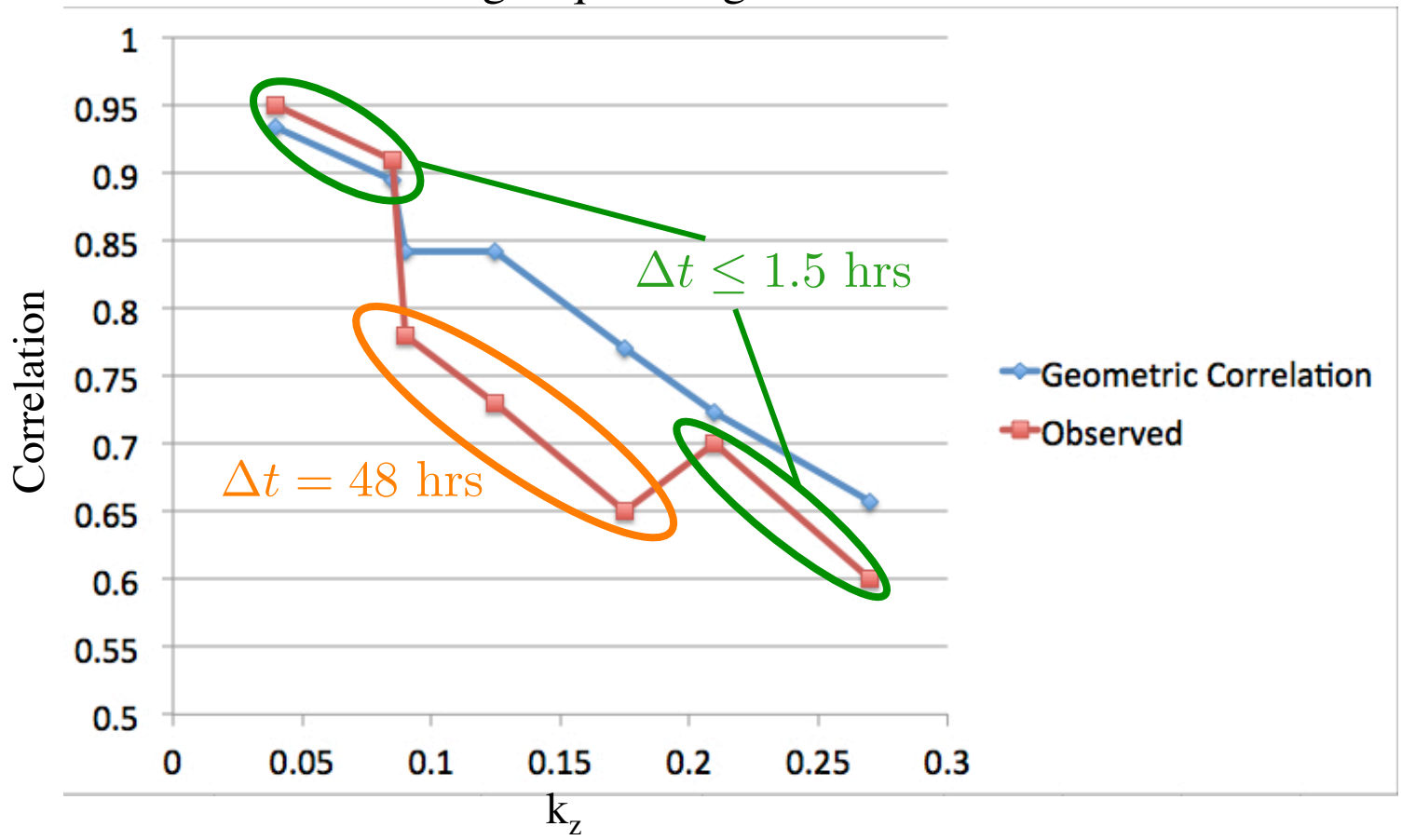

JPL

Enhanced Science Capability

Enhanced Science Capability

- We have been pursuing several items that should increase the science utility of UAVSAR.
  - Multi-squint processing to allow for simultaneous vector deformation and potentially atmospheric mitigation.
  - Long-baseline processing to support PolinSAR and tomographic applications.
  - Stack processing for both PolinSAR and geodetic applications.
    - Reduces the quadratic nature of current RPI processing to a linear problem with two caveats:
      - Not optimal for all pairs.
      - Increased data volume to investigators and ASF. We may trade throughout concerns for data bandwidth and storage issues.
  - Vector deformation.
    - Want to generate vector deformation products for investigators or try to publically release utility for making vector products.

Multi-Squint Observations

- Vector deformation measurements using differential radar interferometry can normally only be obtained by acquiring multiple repeat pass acquisitions from different vantages.
- This prompts one to ask:
  - Is there a way to obtain the full vector deformation using a single repeat pass?
  - Can we estimate something about the tropospheric delay term?
- UAVSAR has the ability to acquire data simultaneously at multiple squint angles thus opening the possibility of obtaining vector deformation measurements.
- Multi-squint interferometric observations my potentially be used to obtain additional vegetation structure measurements.
  - Verify azimuth symmetry assumptions for flat terrain
  - Provide additional vantages over azimuthally sloped terrain
  - Some k_z diversity

Sensitivity Plots

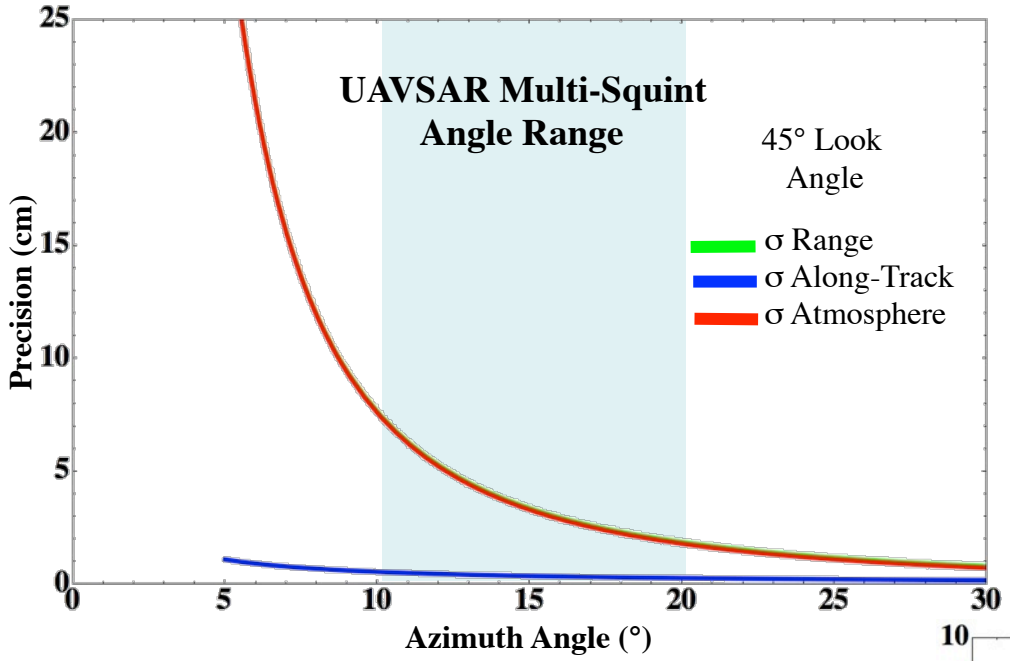

$\gamma = 0.92$

$N_L = 36$ (8 m spatial resolution)

$\lambda = 0.24$ m

- Range and atmospheric precisions are about 5-10 times less sensitive than the along-track component for practical squint angles for UAVSAR and hence require additional filtering.
- Range and atmosphere precisions also exhibit a strong look angle dependence.

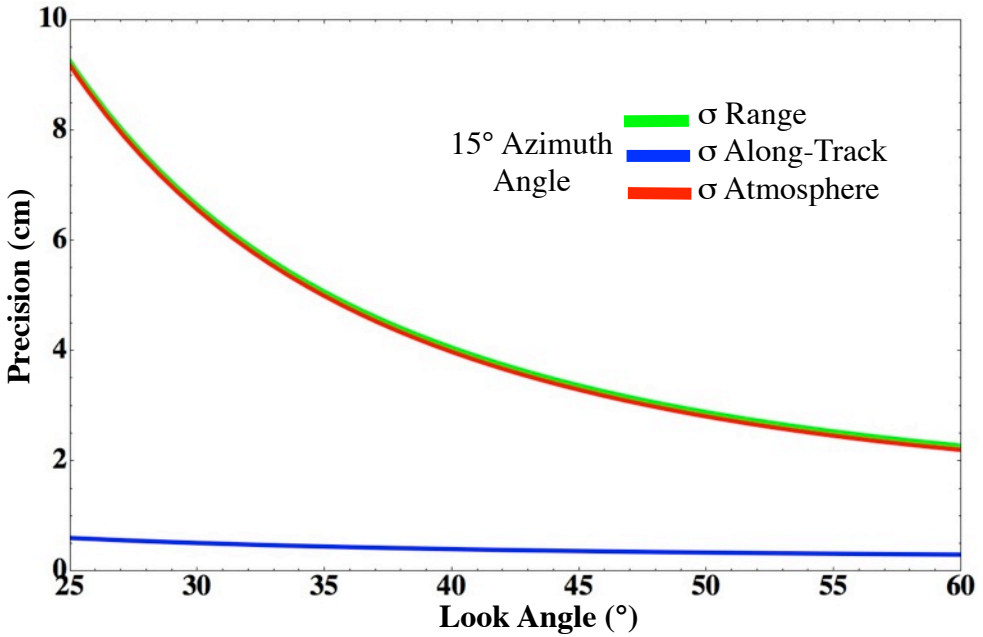

Subsidence Model

- To test the inversion we simulated a subsidence bowl with 10 cm of vertical displacement and 5 cm of radially inward lateral displacement.
- For the atmosphere we assumed a simple -8/3 power law PSD with 0 mean and a 2 cm standard deviation.

$$\vec{d}_{enu} = \begin{bmatrix} -L_m \sin\left[\frac{\pi(e-e_o)}{r_b}\right] \\ -L_m \sin\left[\frac{\pi(n-n_o)}{r_b}\right] \\ \frac{(u_t-u_b)}{2\tanh s_f} \tanh\left[\frac{2s_f(r-r_f)}{r_b-r_f} - s_f\right] \frac{u_t+u_b}{2} \end{bmatrix}$$

Parameter	Value
Flank Radius (r_f)	1.5 km
Bowl Radius (r_b)	10 km
Lateral Displacement (L_m)	5 cm
Steepness Factor (s_f)	2.3
Vertical Rim (u_t)	0
Vertical Center (u_b)	-10 cm

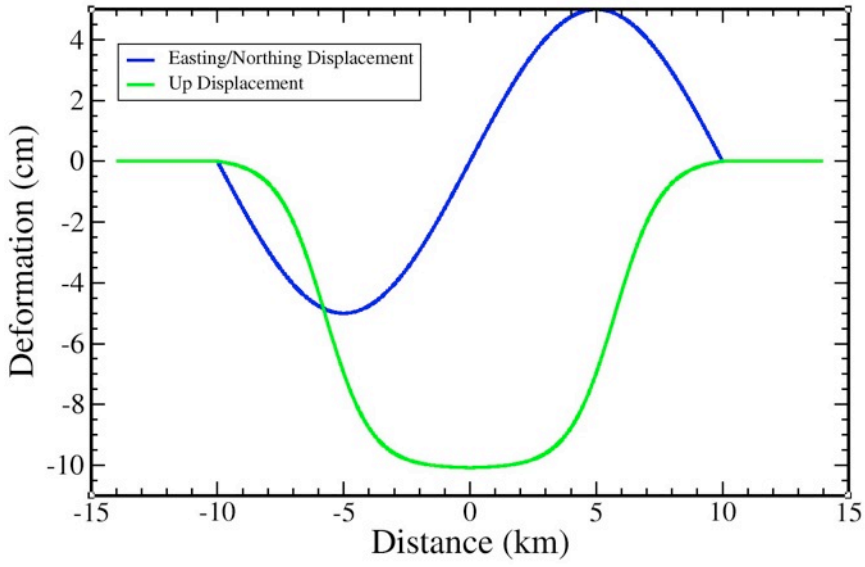

Subsidence Bowl Deformation

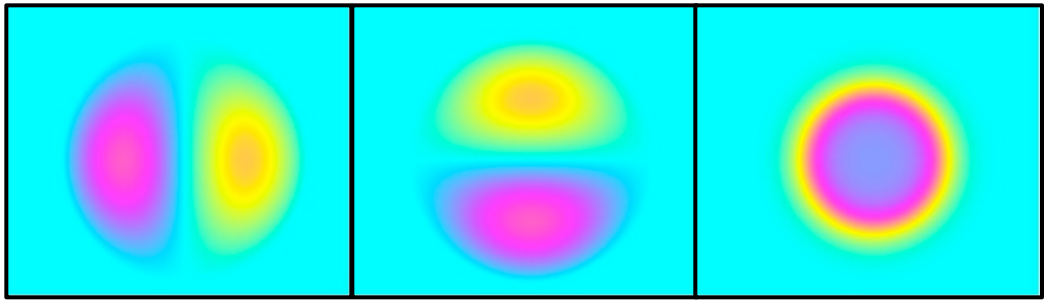

East North Up

12 cm color wrap

Simulation Results

- Results of the inversion for the subsidence bowl assuming a 0.92 interferometric correlation. Precision results follow the model.

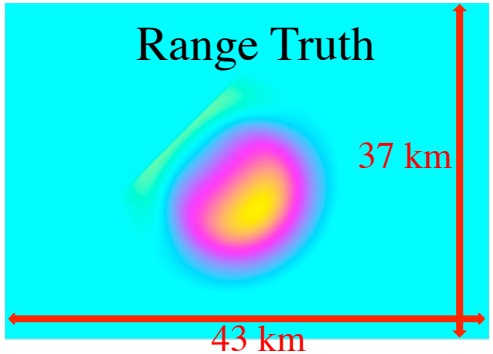

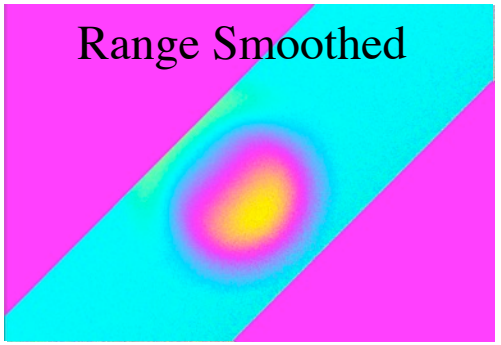

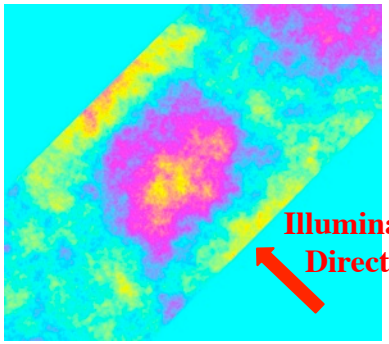

Broadside
Line-of-Sight
Measurement

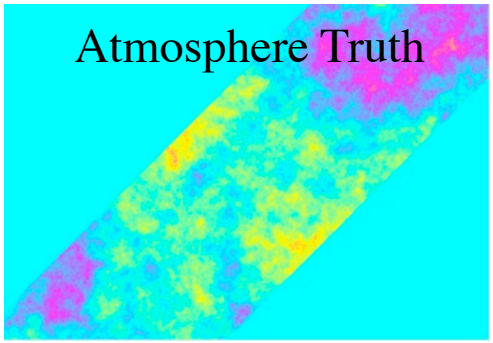

- Test with actual data so far have not yielded good results to date. Continuing testing.

Magnitude and Correlation for θ_{az}=0°

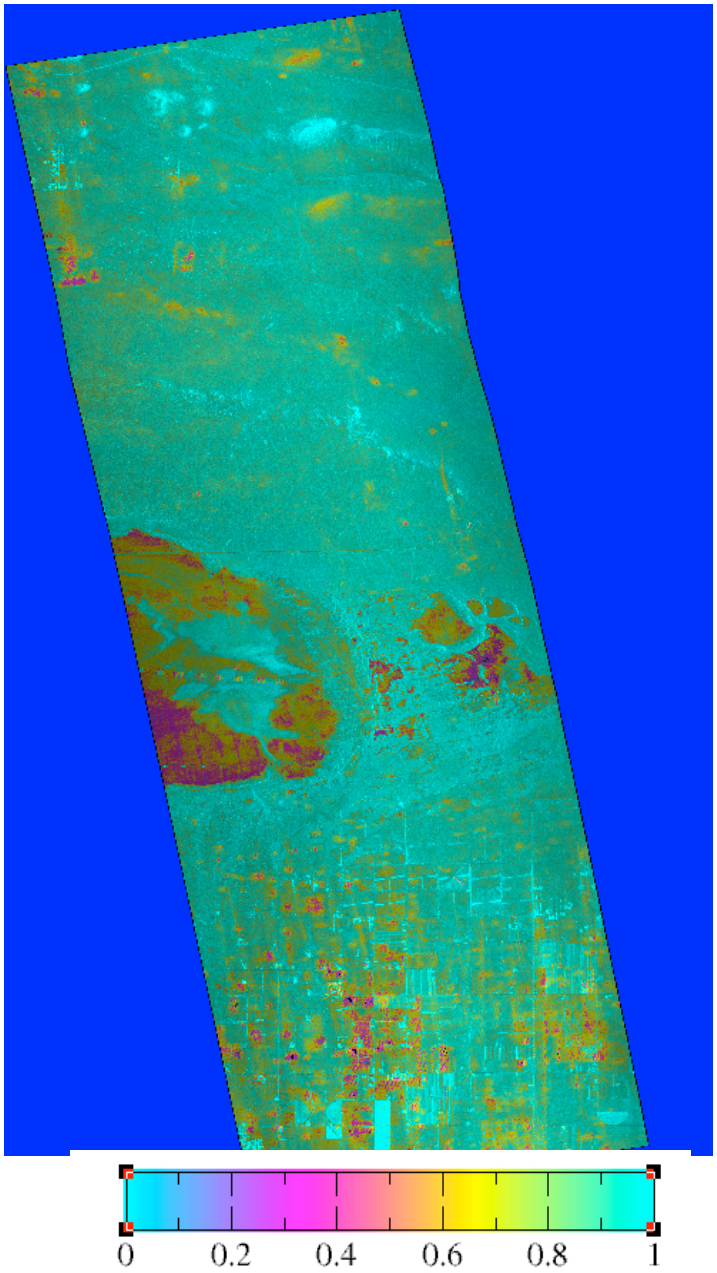

- UAVSAR collected three passes of fully polarimetric multi-squint data with an azimuth steering angle of ±15°.
- Data was collected at a heading of 350° at the UAVSAR nominal flying altitude of 12.5 km over the Rosamond Dry Lake Bed calibration site in California.
- Region is located in Mojave Desert with a urban area in southern section of the scene.
- Time interval between multi-squint observations is approximately 20-25 sec.

I

Multi-Squint Correlation Files

- Correlation for the three azimuth angles for passes 1 and 2 with a 26 minute separation.

$\theta_{az} = 15°$ $\theta_{az} = 0°$ $\theta_{az} = -15°$

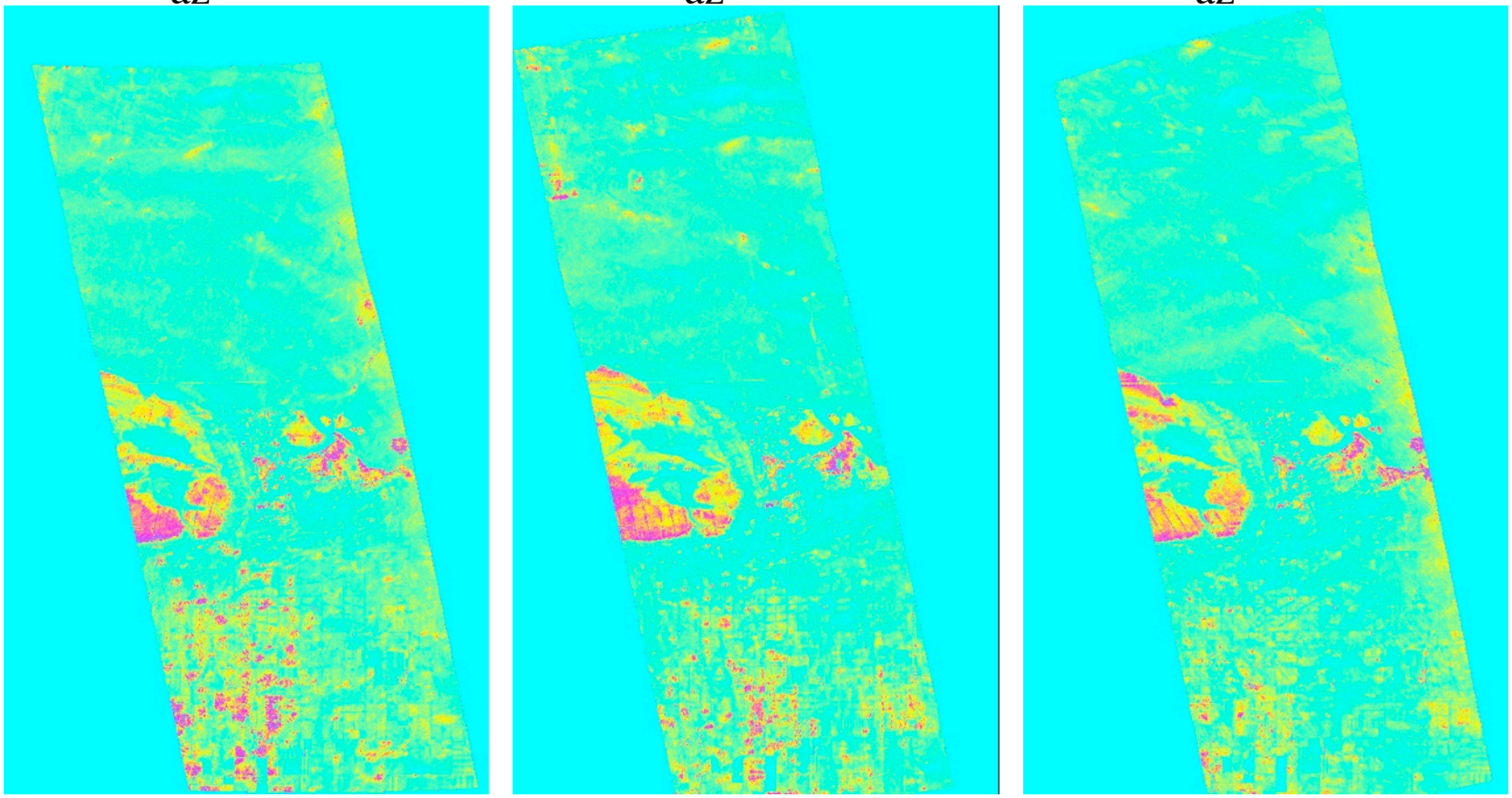

Multi-Squint Interferograms

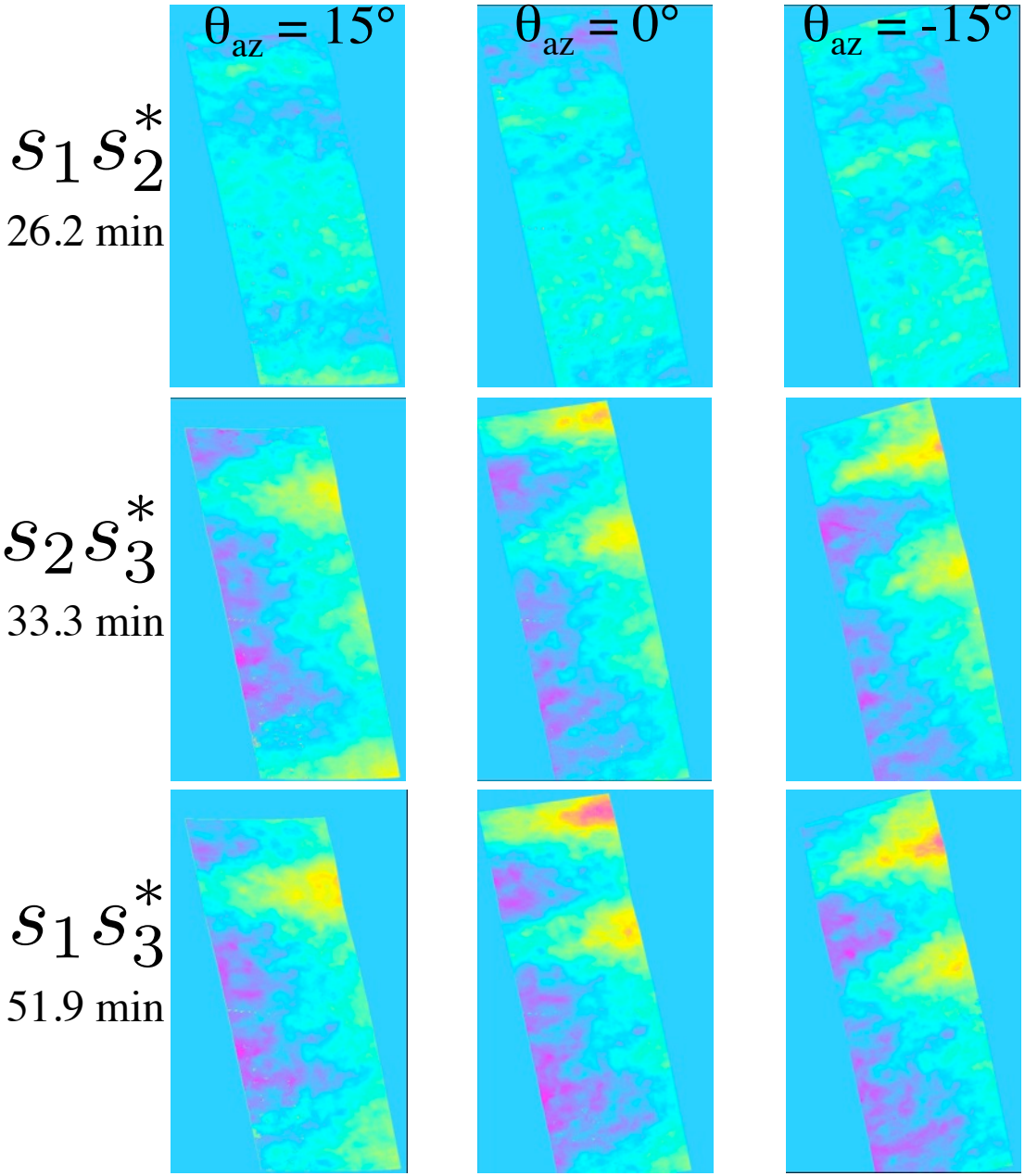

Time Between Passes

1-2 26.2 min
2-3 33.3 min
1-3 51.9 min

Data collected July 10, 2010

Multi-Squint Deformations

Range Solution

Along-Track Solution

Atmosphere Solution

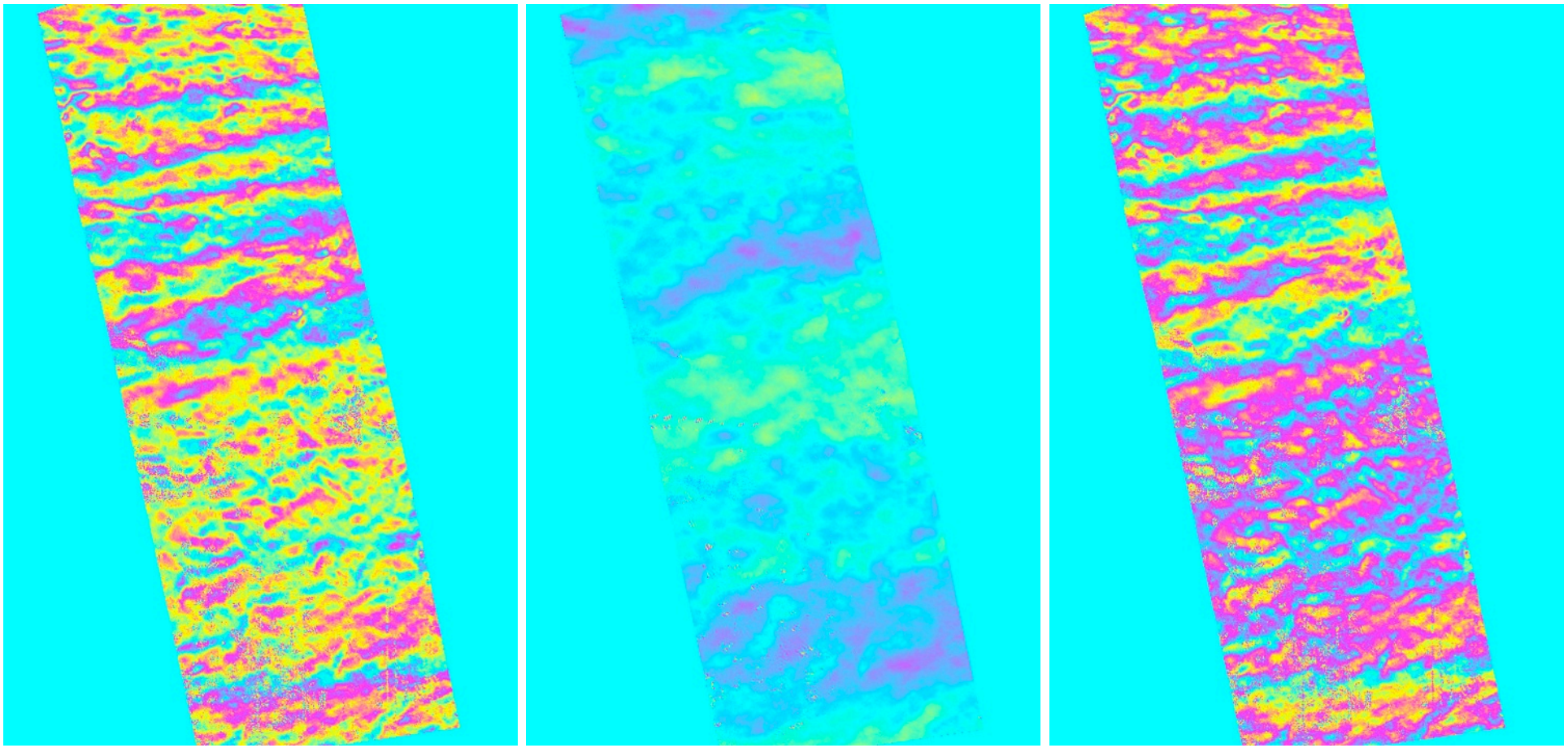

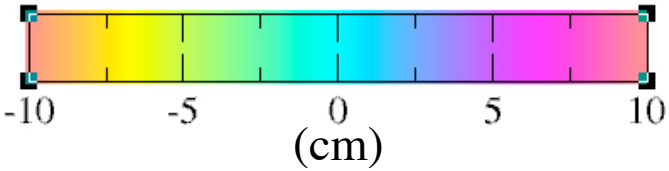

JPL

Science Results

Landslide Motion Detection Near Parkfield, CA

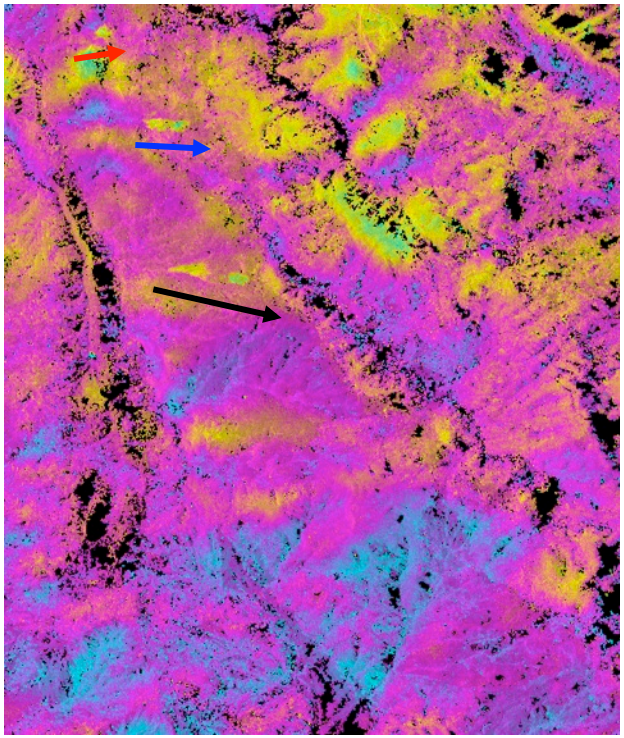

- Creeping landslides detected in 31 and 80 day repeat pass interferograms.
- The amount of deformation increased for the larger pair with the larger temporal baseline indicating continued creep from May to July 2008.

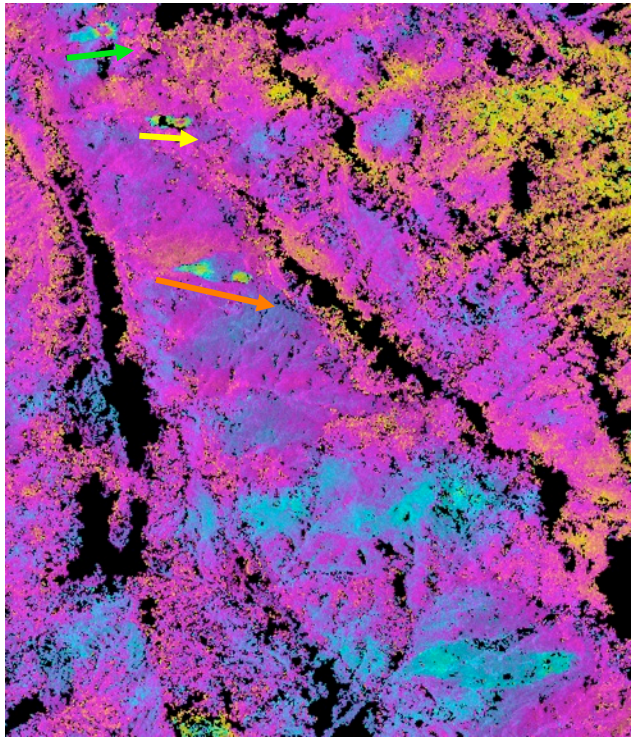

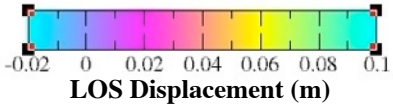

31 Day Repeat

80 Day Repeat

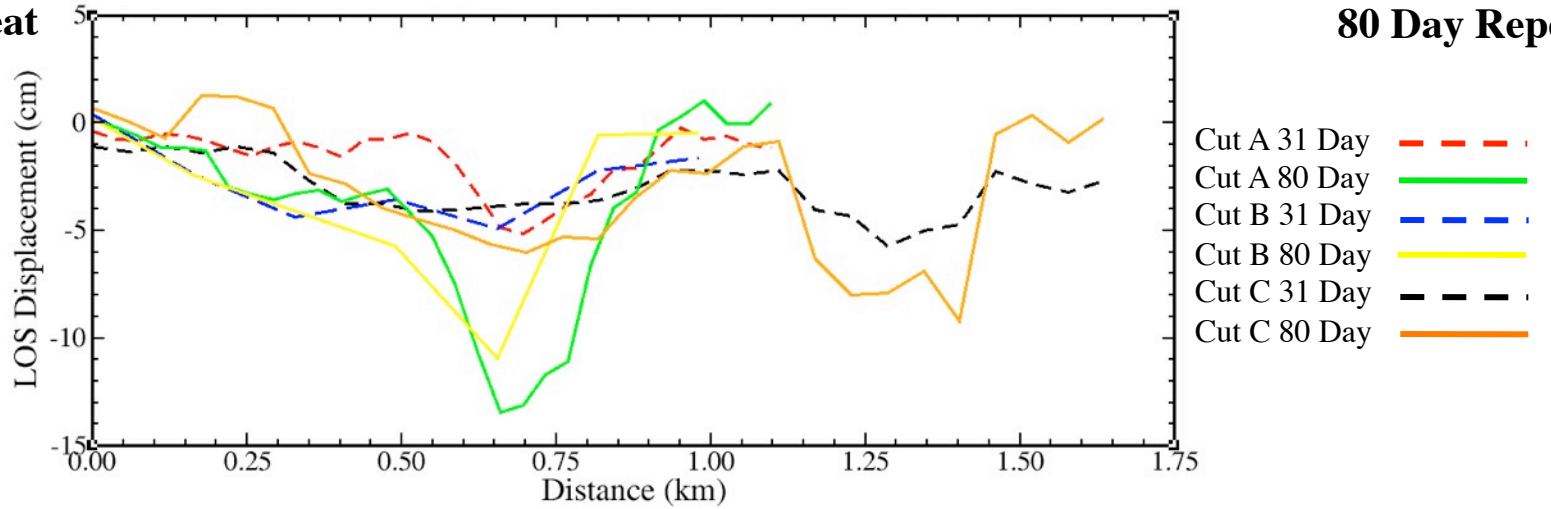

HH Correlation Greater Than VV

- Although the polarization signatures look very similar on the two dates we see areas that are well correlated at HH but very decorrelated for VV polarization.

March 25, 2008
Polarimetric Image

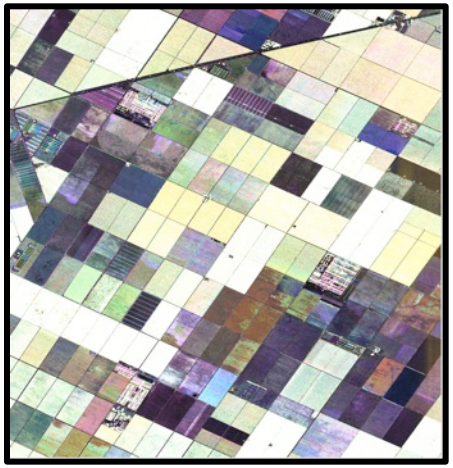

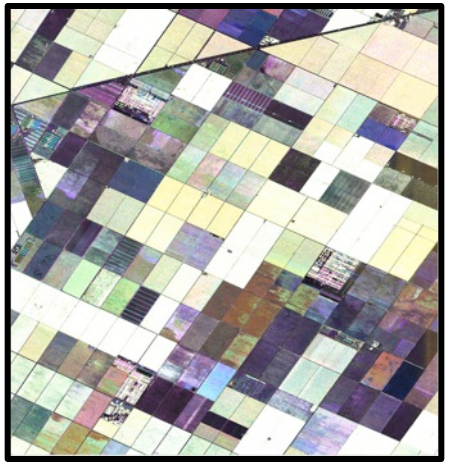

March 31, 2008
Polarimetric Image

HH Correlation

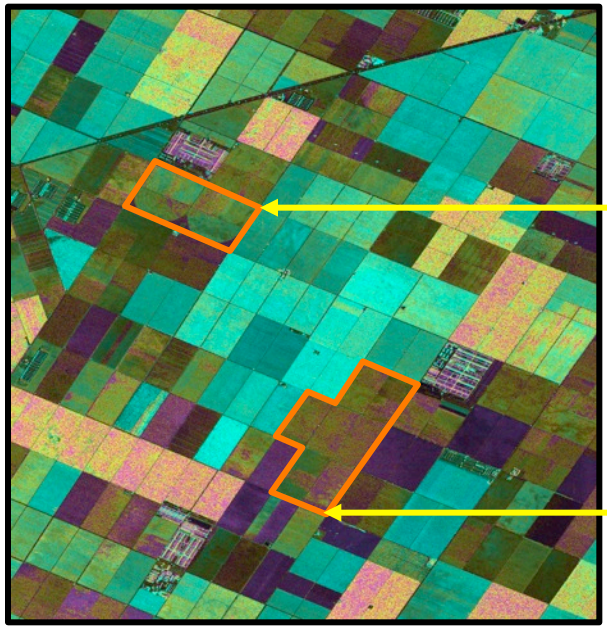

- Outlined regions have better HH correlation than VV correlation even though surrounding fields are nearly identical for HH and VV correlation.

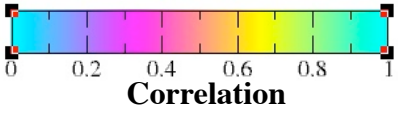

VV Correlation

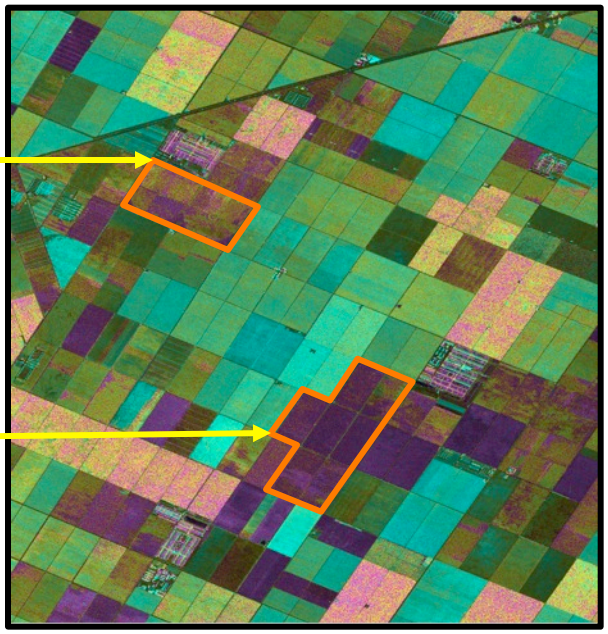

VV Correlation Greater Than HH

- Converse to the previous example there are regions that are better correlated at VV than HH.

HH Correlation

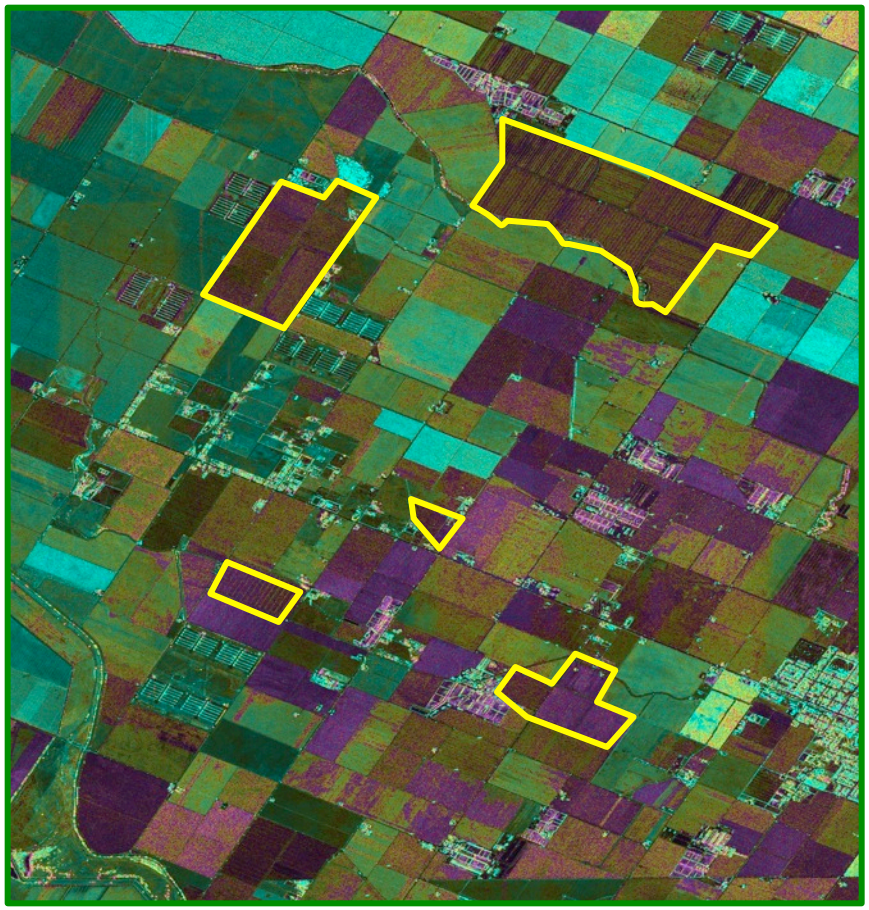

VV Correlation

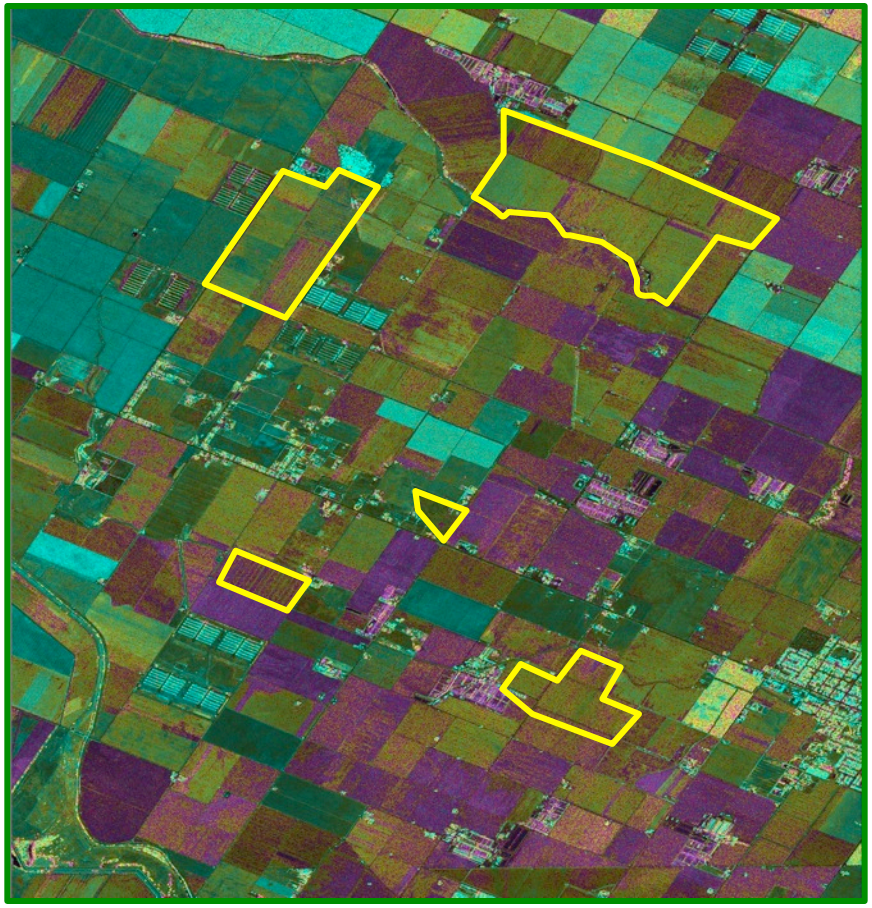

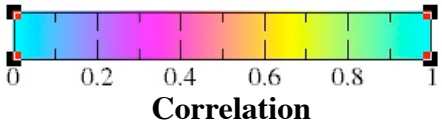

E5 Site Photos – June 2010

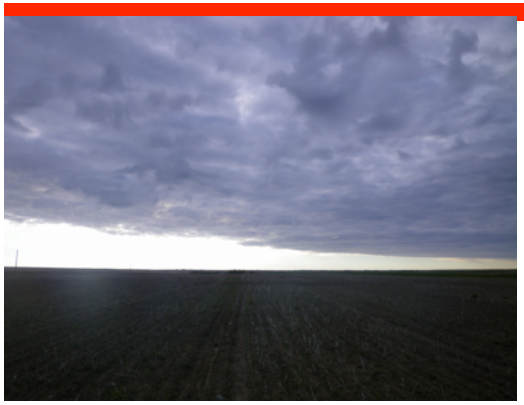

June 2

June 9

June 13

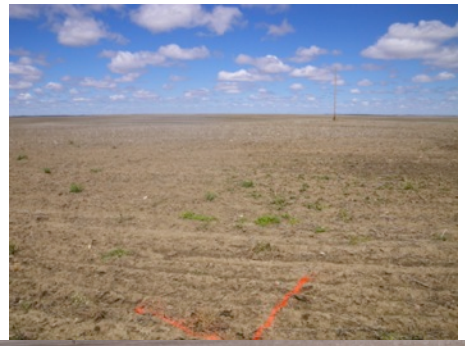

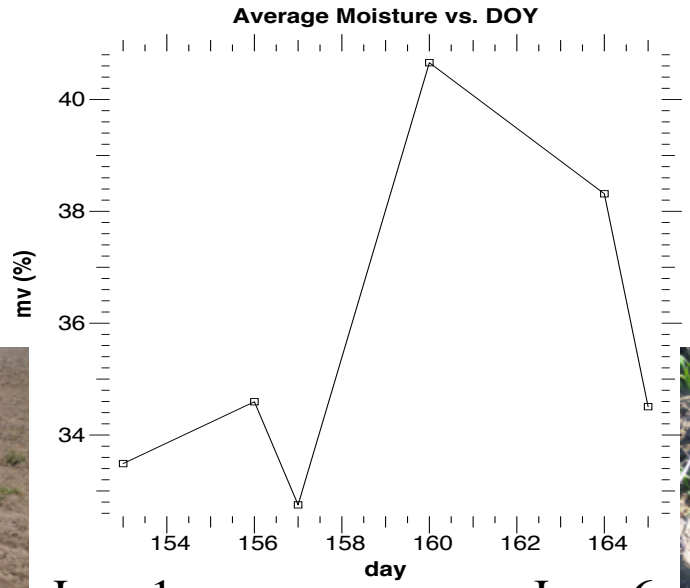

June 1

June 6

Photos Courtesy of Brenda Toth

VV Correlation

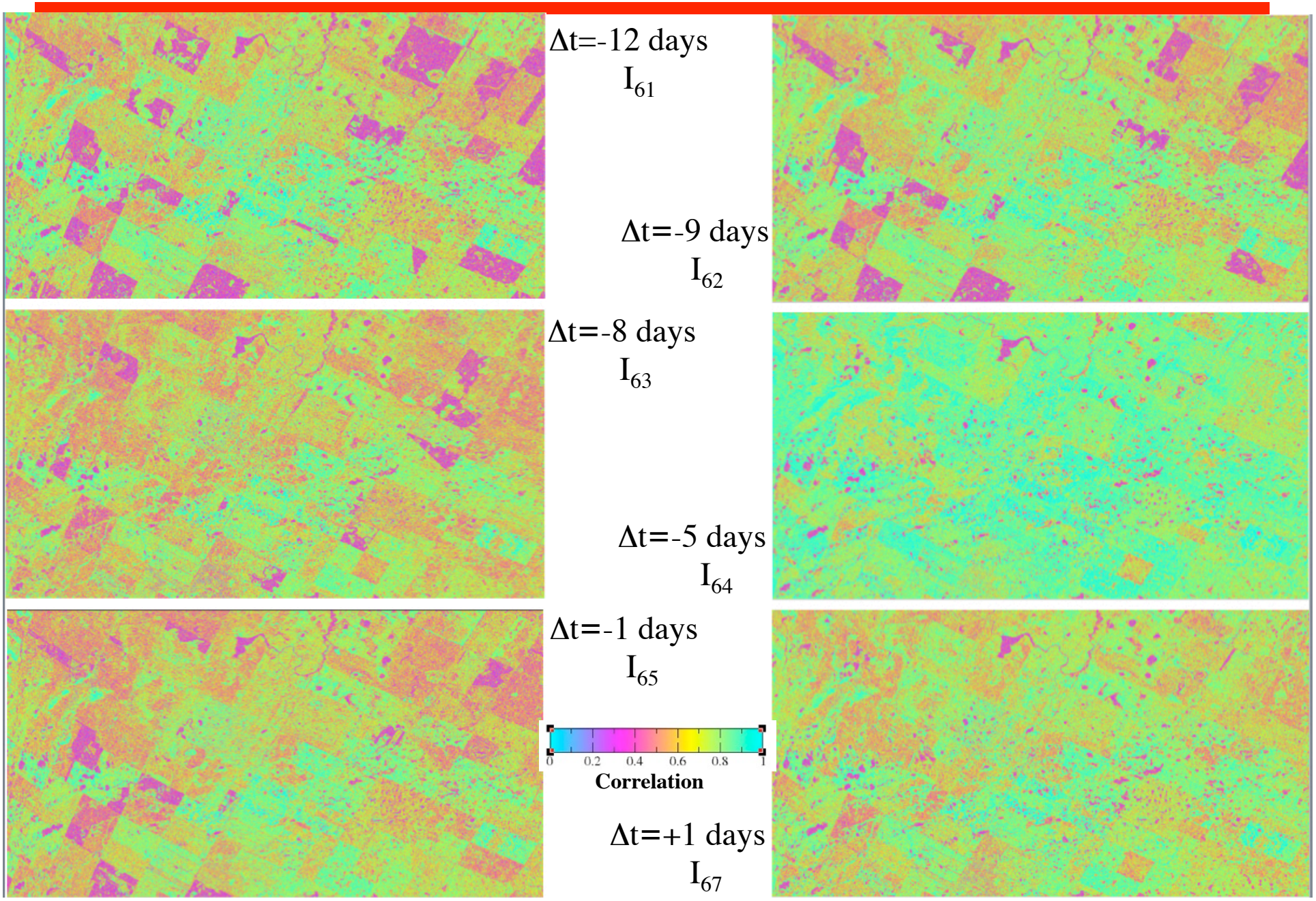

HH Interferograms

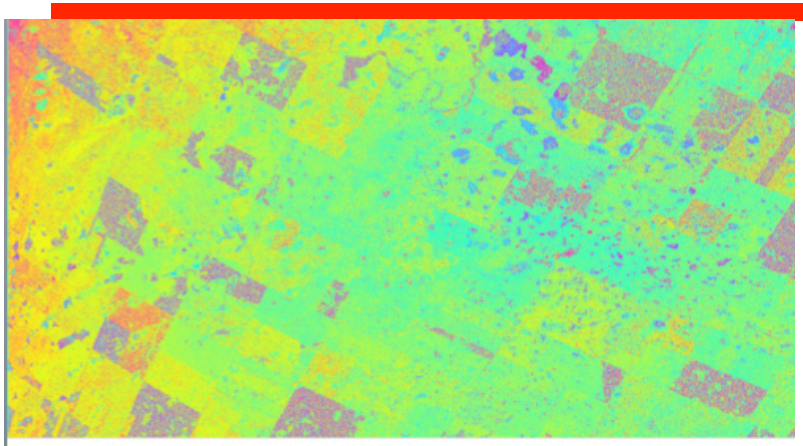

Δt=-12 days

I_{61}

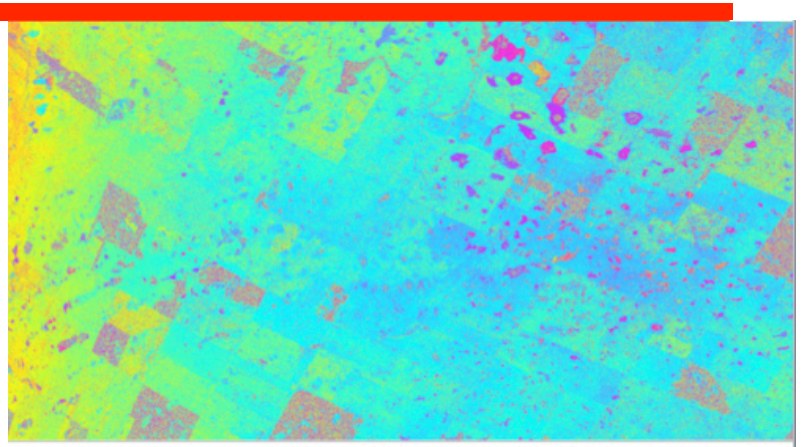

Δt=-9 days

I_{62}

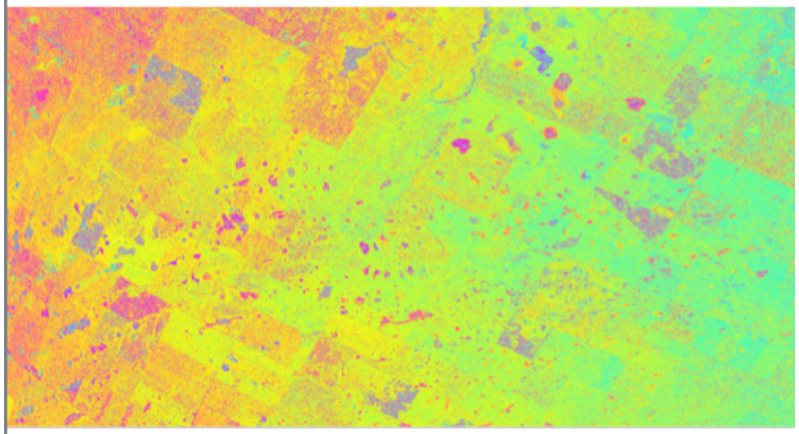

Δt=-8 days

I_{63}

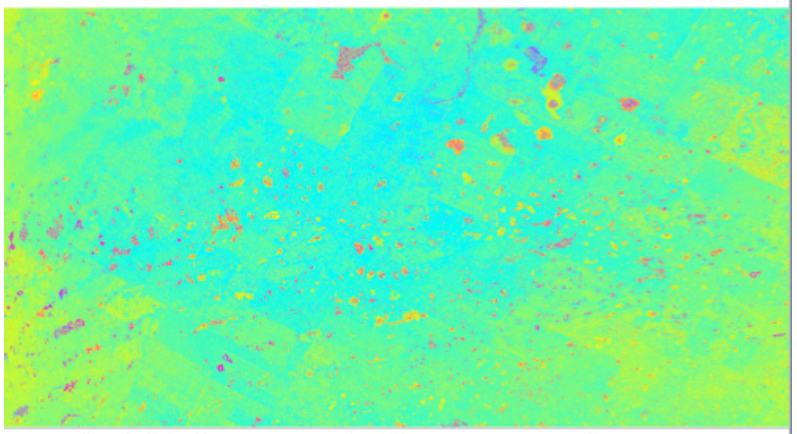

Δt=-5 days

I_{64}

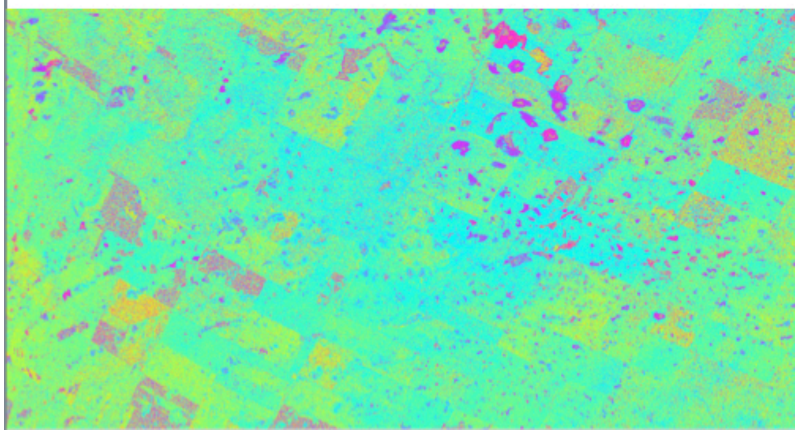

Δt=-1 days

I_{65}

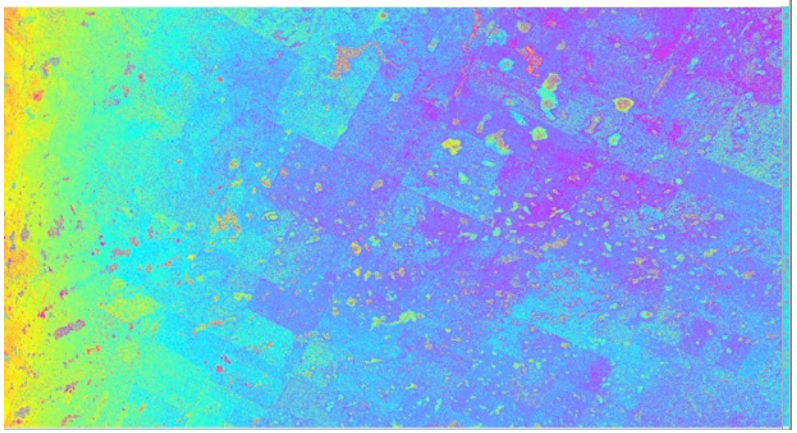

Δt=+1 days

I_{67}

Interferometric Correlation Versus Δm_v

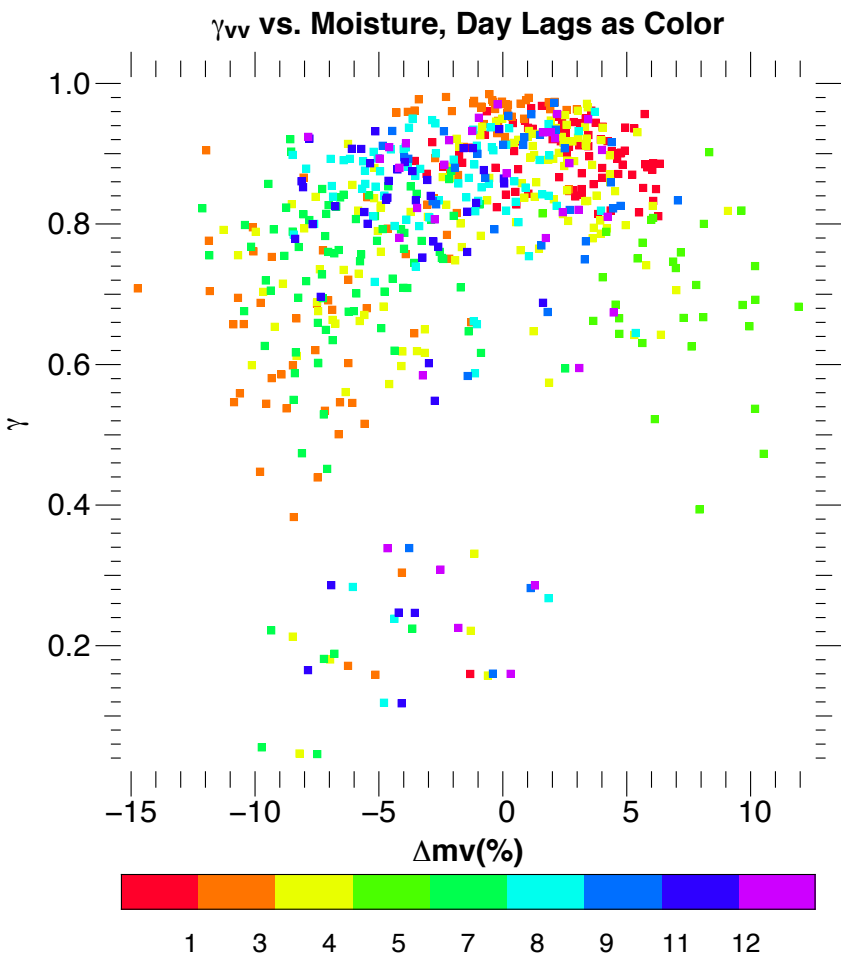

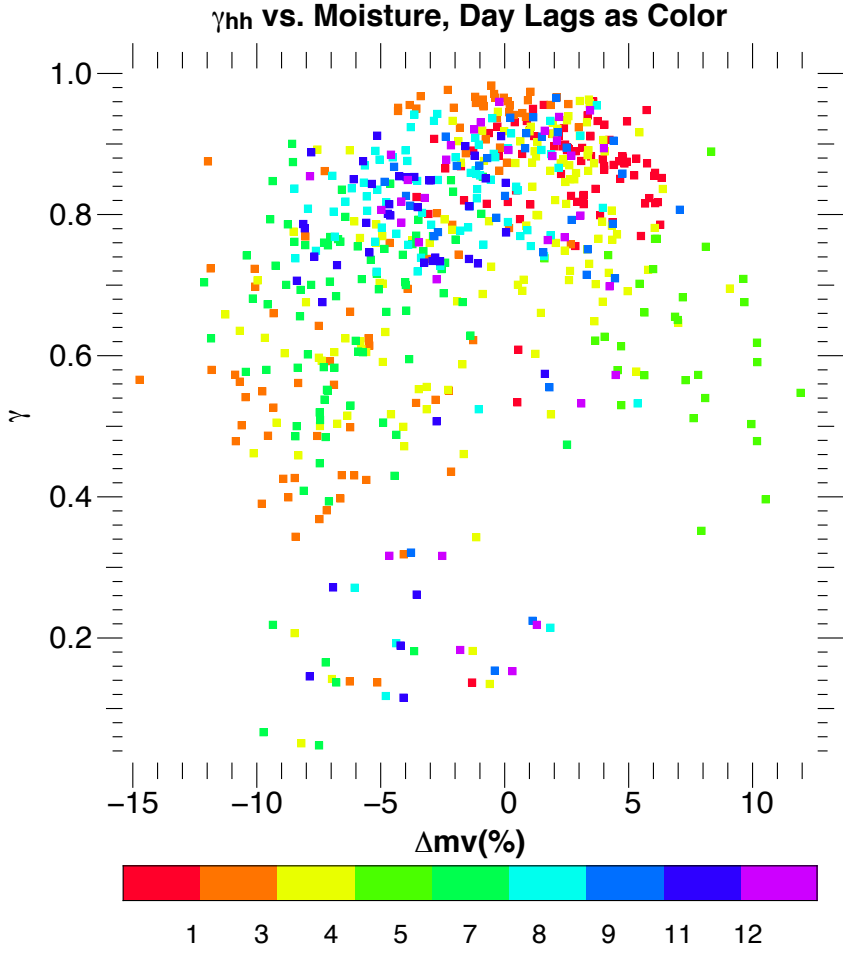

- Average HH and VV correlation over the *in situ* measurement sites versus change in soil moisture.

- Note, the correlation tends to decrease more for larger changes in soil moisture indicating soil moisture is effecting the interferometric measurement.

HH/VV Differential Interferograms

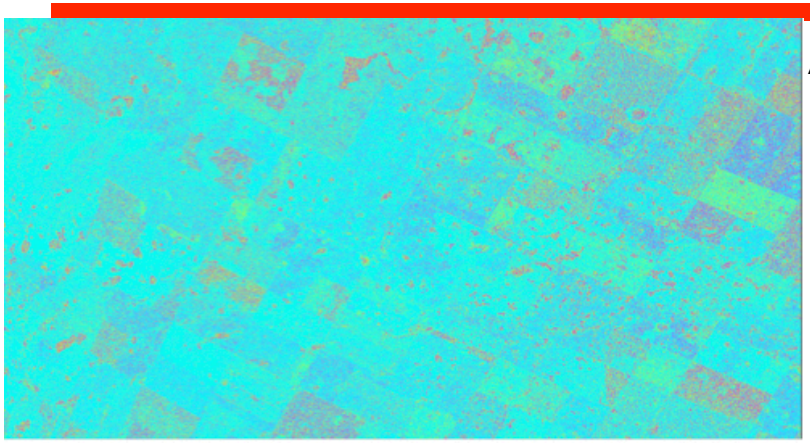

Δt=-12 days

I_{61}

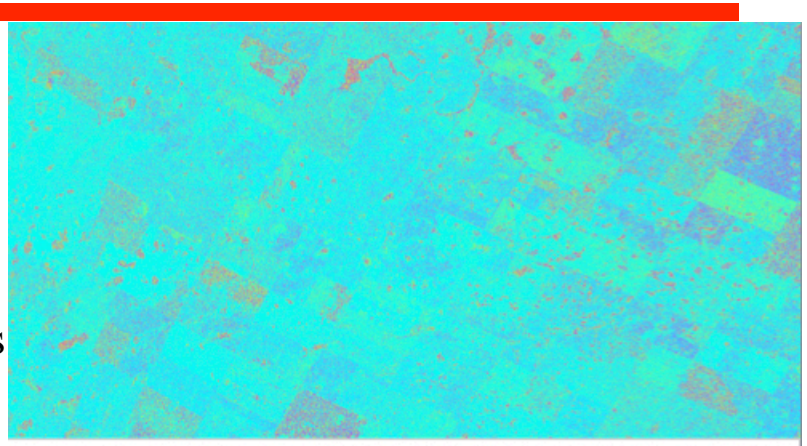

Δt=-9 days

I_{62}

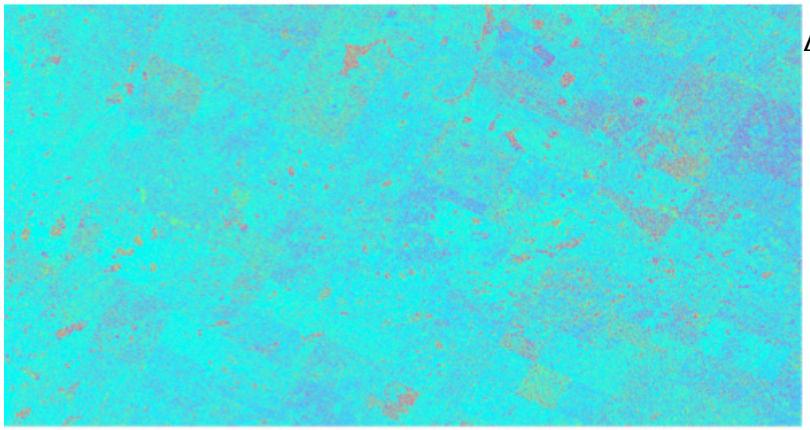

Δt=-8 days

I_{63}

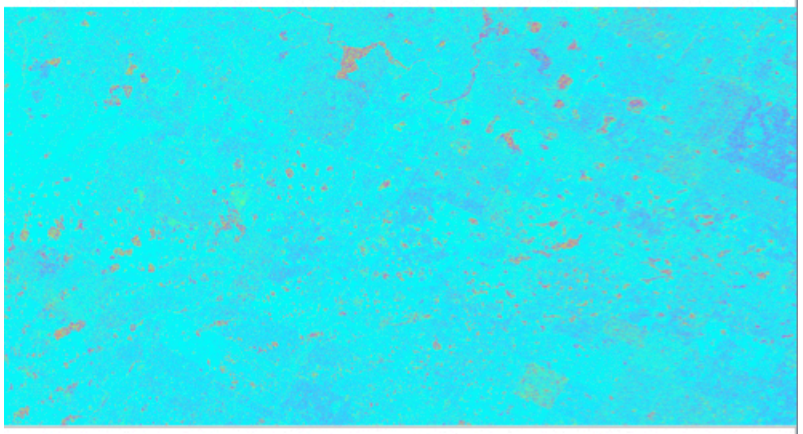

Δt=-5 days

I_{64}

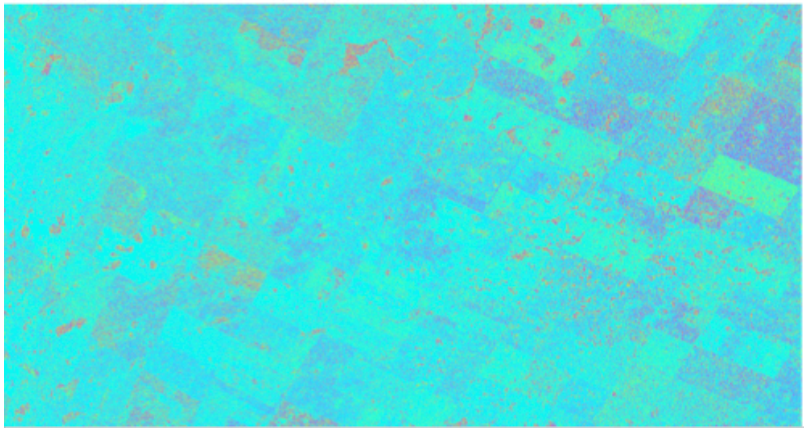

Δt=-1 days

I_{65}

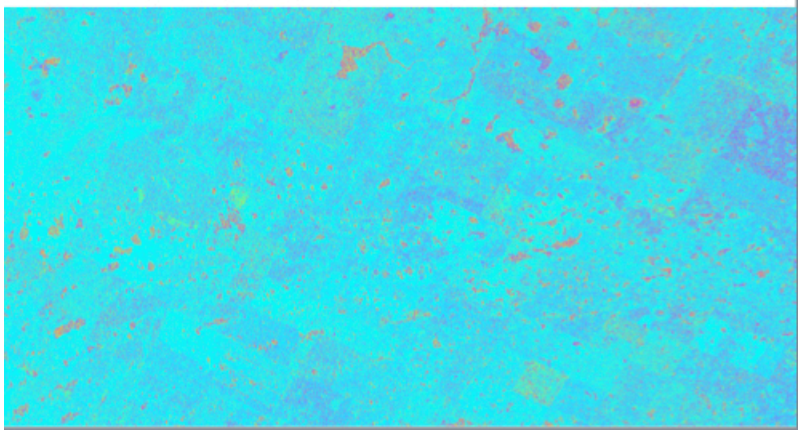

Δt=+1 days

I_{67}

Oh Model VV Phase vs Measurements

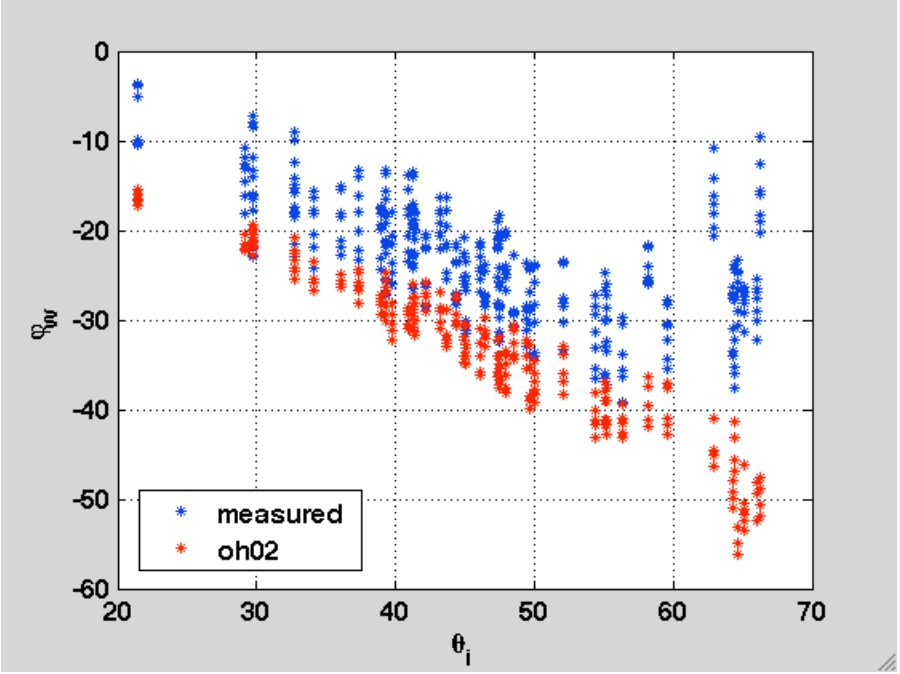

- Oh model VV polarimetric phase versus and measured VV polarimetric phase plotted versus incidence angle.
- There is good agreement with the trend except at high incidence angles and there is a slight bias of about 5°.
- Predicted spread from soil moisture is much less in predicted phase than in observed phase (about a factor of 2).

- Scatter plot of measured VV polarimetric phase versus Oh model polarimetric phase.
- Models agree reasonably well expect at high incidence angles (greater than 60°).

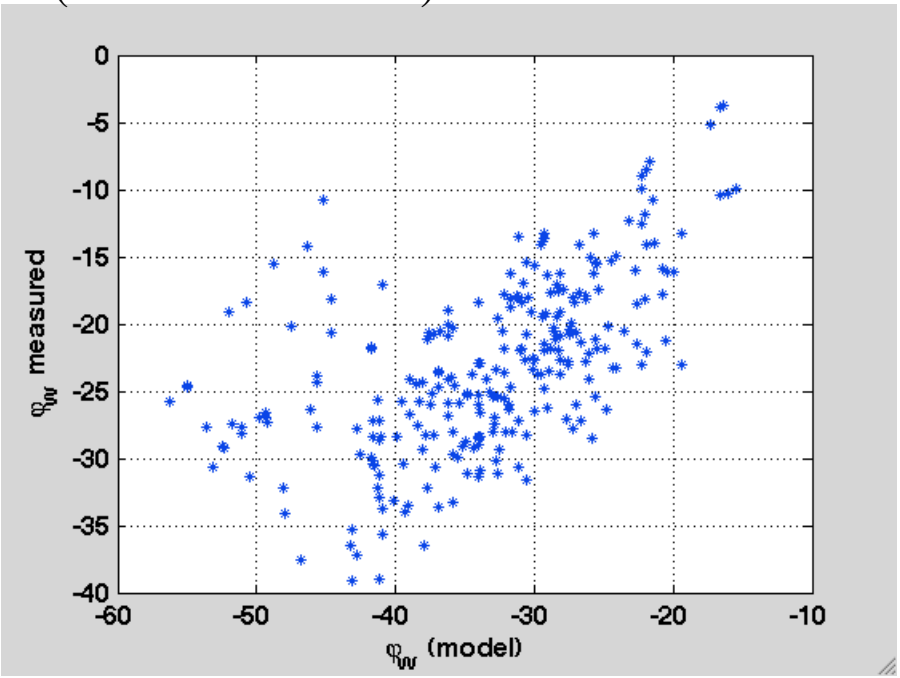

Polarimetric-Interferometric Studies at La Amistad International Park

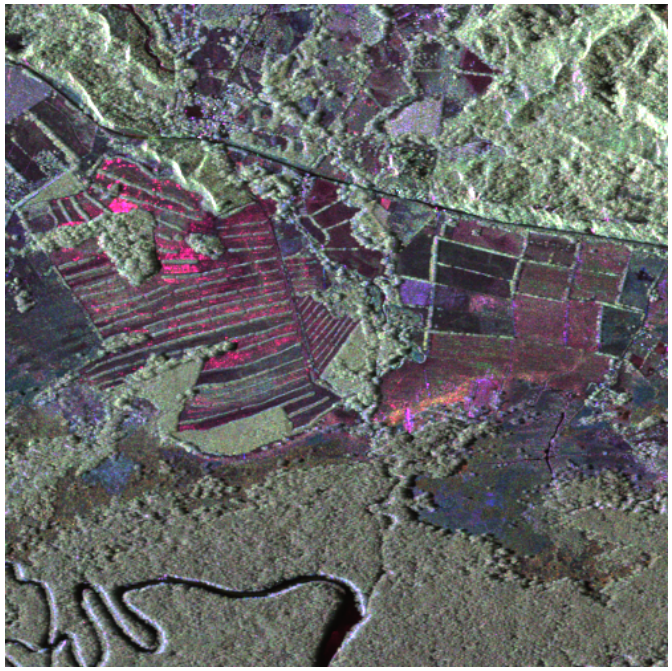

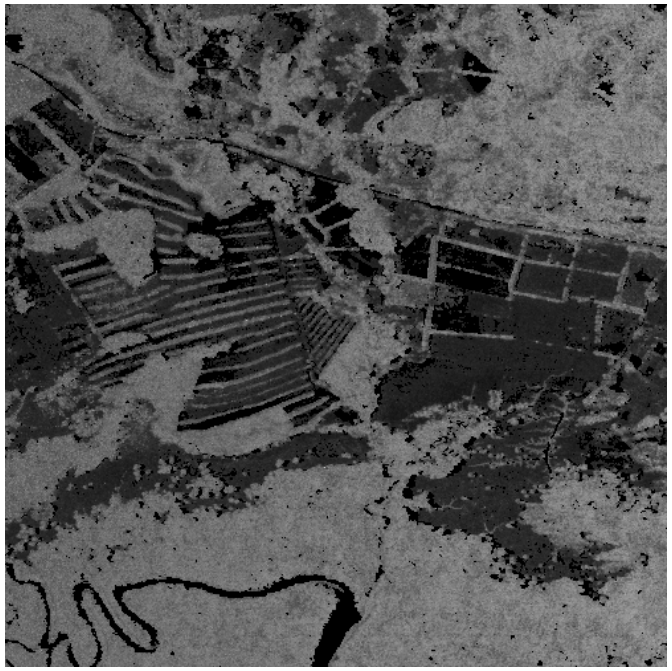

by

Scott Hensley, Maxim Neumann, Thierry Michel, Marco Lavalle,
Bruce Chapman, Ron Muellerschoen, and Razi Ahmed

January 29, 2013

POLINSAR 2013 WORKSHOP

Frascati, Italy

UAVSAR Data Collections La Amistad

- On February 8, 2010 UAVSAR collected a series of repeat pass lines with a variety of physical baselines. Baseline lengths varied from 20 m to 750 m.
- Data were collected from coast to coast to cover a wide range of biomes and terrains.
- Data were collected on opposite headings for look direction diversity.

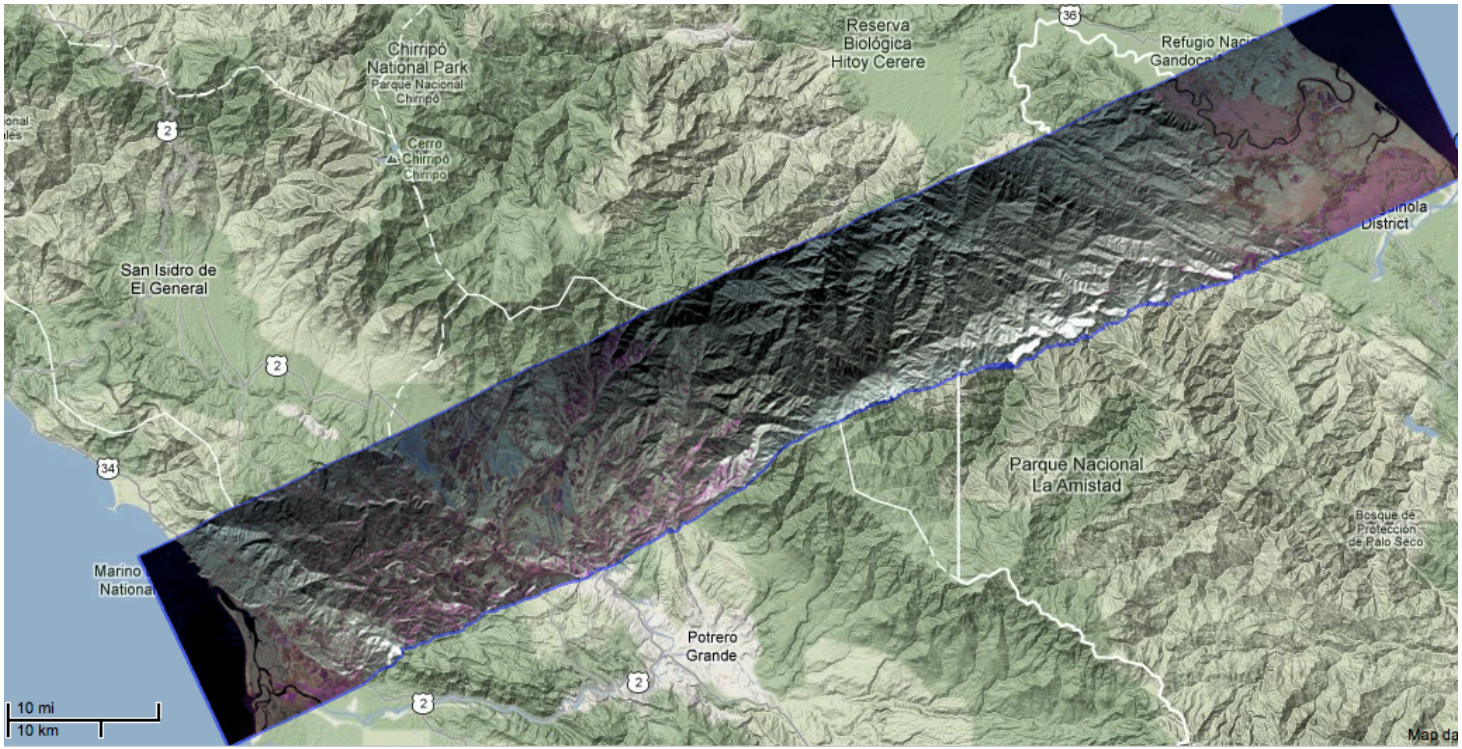

Initial Study of La Amistad

- For our initial analysis we processed the short physical baseline pairs with lengths less than 100 m. This consisted of 5 tracks for a total of 10 interferometric pairs with physical baselines ranging from 1.6 to 100 m.
- Temporal baselines ranged from an half hour to three hours.
- From these pairs we picked 6 regions spanning a range of biomes, terrain types and incidence angle.
- Our initial study goals are:
  - Understand the variability of temporal correlation for short time repeat pass pairs in a tropical environment.
  - Check to consistency of PolinSAR inversions for a single baseline.

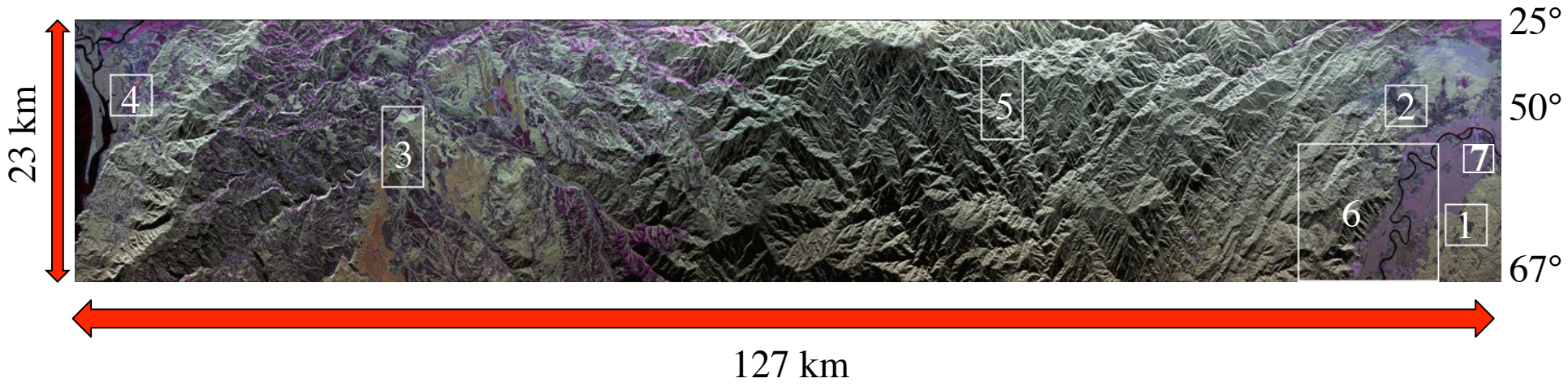

Physical/Temporal Baselines

Physical Baselines (m)

Track #	1	2	3	4	5
1		1.6	19.0	79.1	99.4
2			19.2	79.4	99.7
3				60.2	80.5
4					20.3
5					

Temporal Baselines (hr)

Track #	1	2	3	4	5
1		3.2	0.7	1.3	1.9
2			-2.6	-1.9	-1.3
3				0.7	1.3
4					0.6
5					

Tree Heights in La Amistad

- Tree heights at the 1 km scale derived by Marc Simard using IceSAT lidar are shown in the map below.
  - Largest tree height in 1 km cell

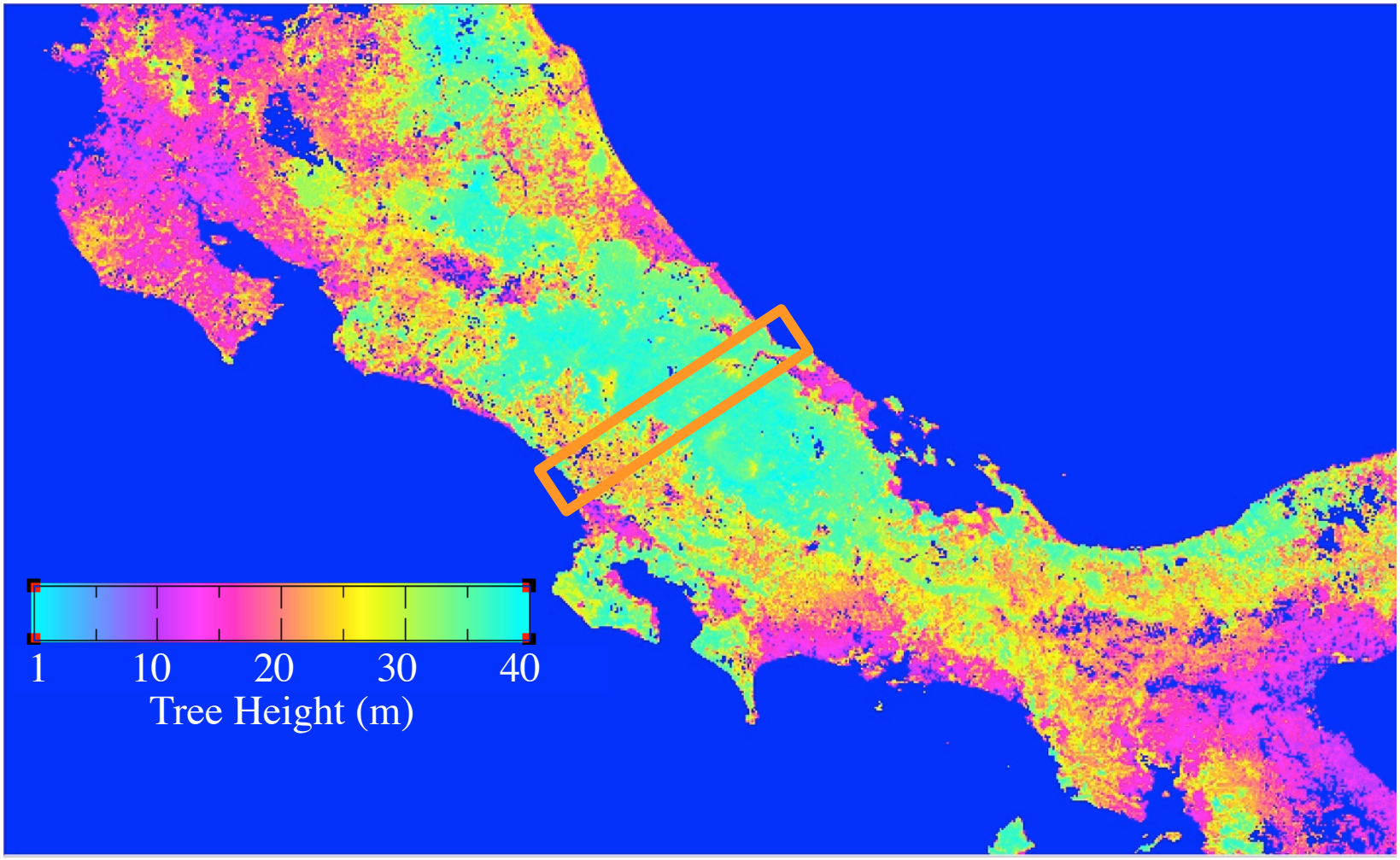

Baseline Summary Table and Nomenclature

c_t	r_t	Baseline #	Baseline Length	Temporal Interval
2	1	0	1.6	3.2
3	1	1	19.0	0.7
3	2	2	19.2	-2.6
4	1	3	79.1	1.3
4	2	4	79.4	-1.9
4	3	5	60.2	0.7
5	1	6	99.4	1.9
5	2	7	99.7	-1.3
5	3	8	80.5	1.3
5	4	9	20.3	0.6

Long Temporal Baseline

Short Physical Baseline

"Good Baselines"

Short Physical Baseline

	1	2	3	4	5
1		0	1	3	6
2			2	4	7
3				5	8
4					9
5					

$$b_{\#} = \frac{(c_t - 1)(c_t - 2)}{2} + r_t - 1$$

Correlation on Bare Surfaces

- Most bare surfaces stayed well correlated during the 3 hours spanning the data collection period.

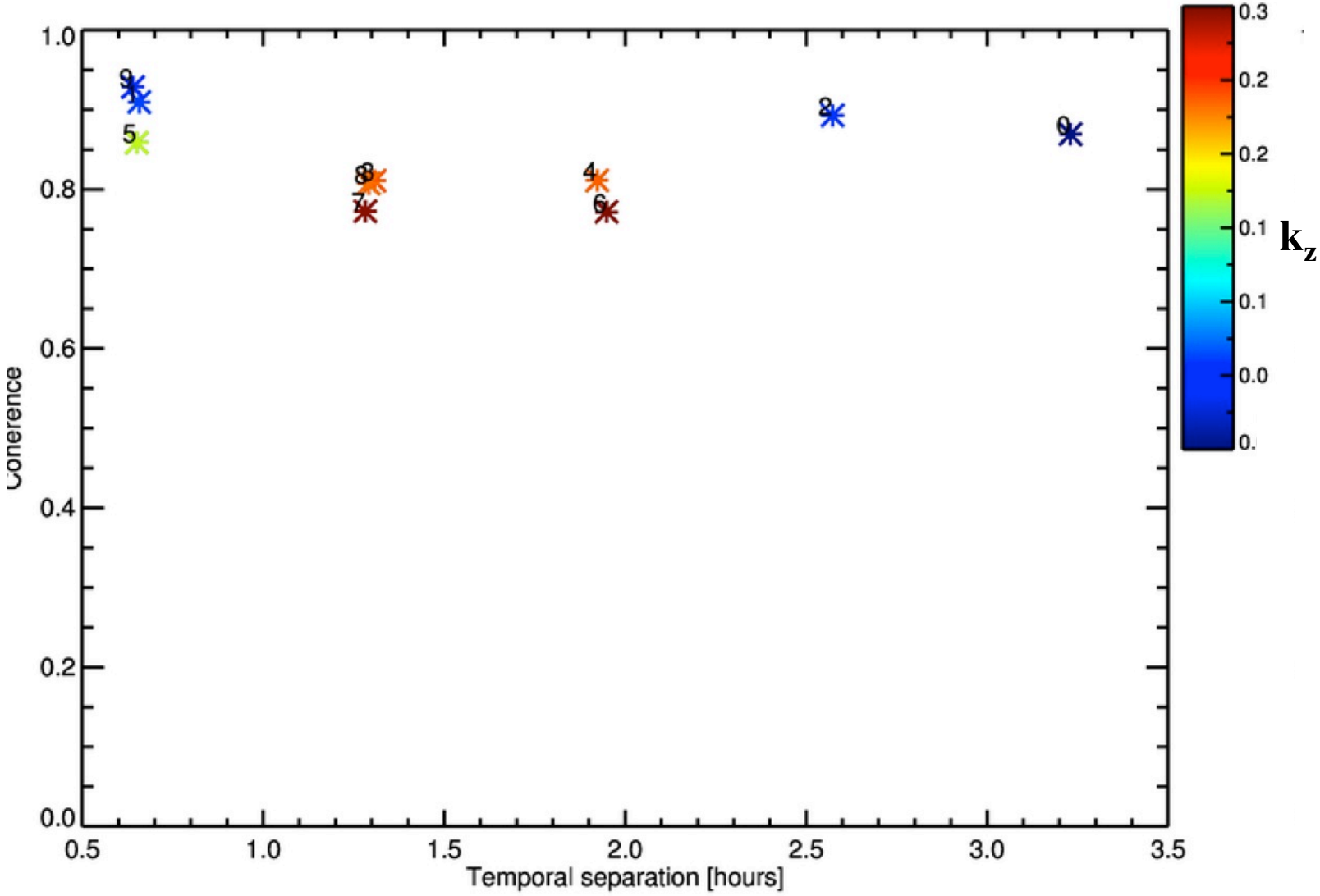

Correlation in Forested Areas – k_z

- Correlation in forested areas as a function of k_z.

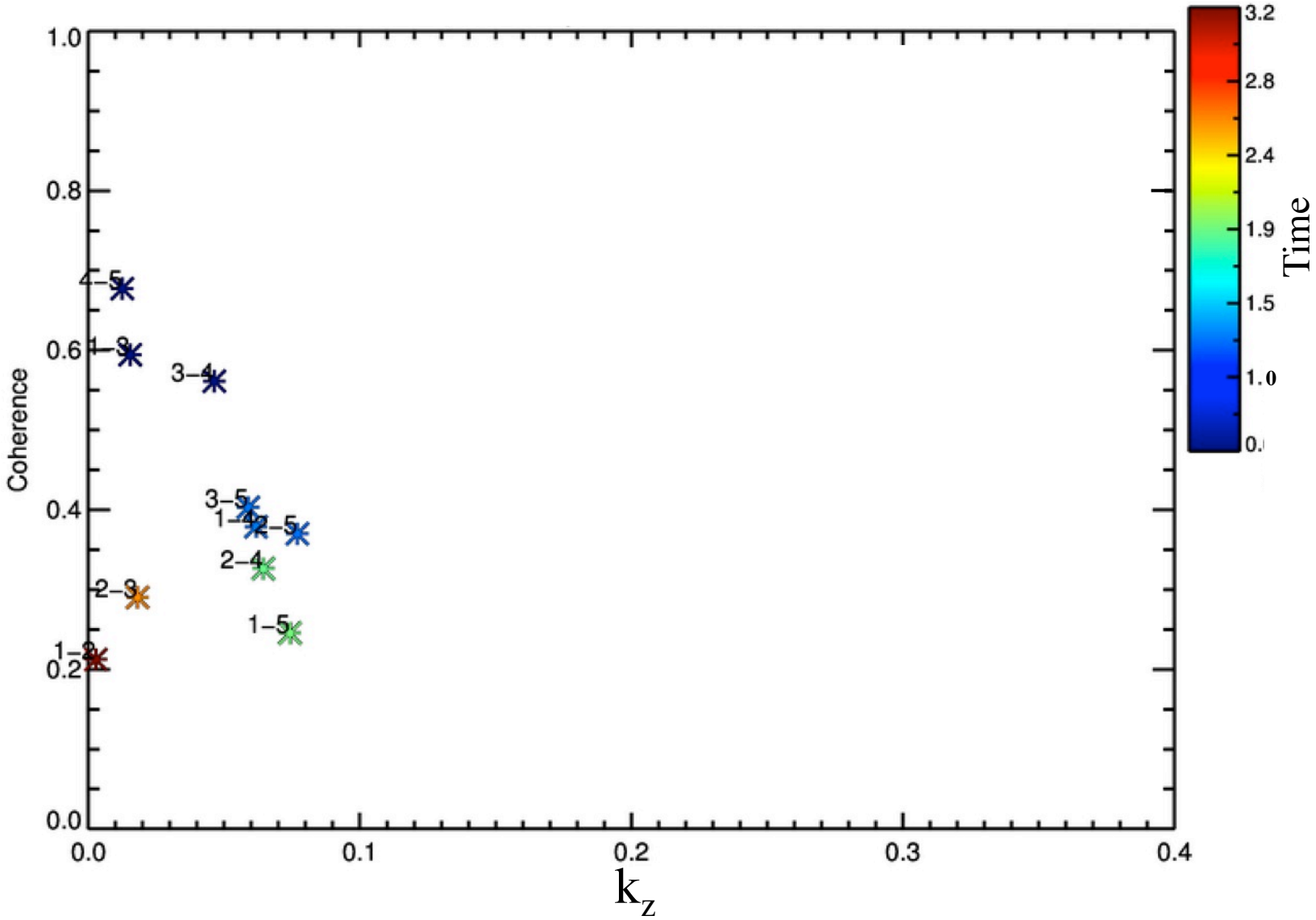

Correlation in Forested Areas – Time

- Temporal decorrelation at La Amistad is substantial even for temporal baselines as short as a couple of hours. On the Δt=3 hour pair temporal decorrelation exceeded volumetric correlation even for the long baseline pairs.

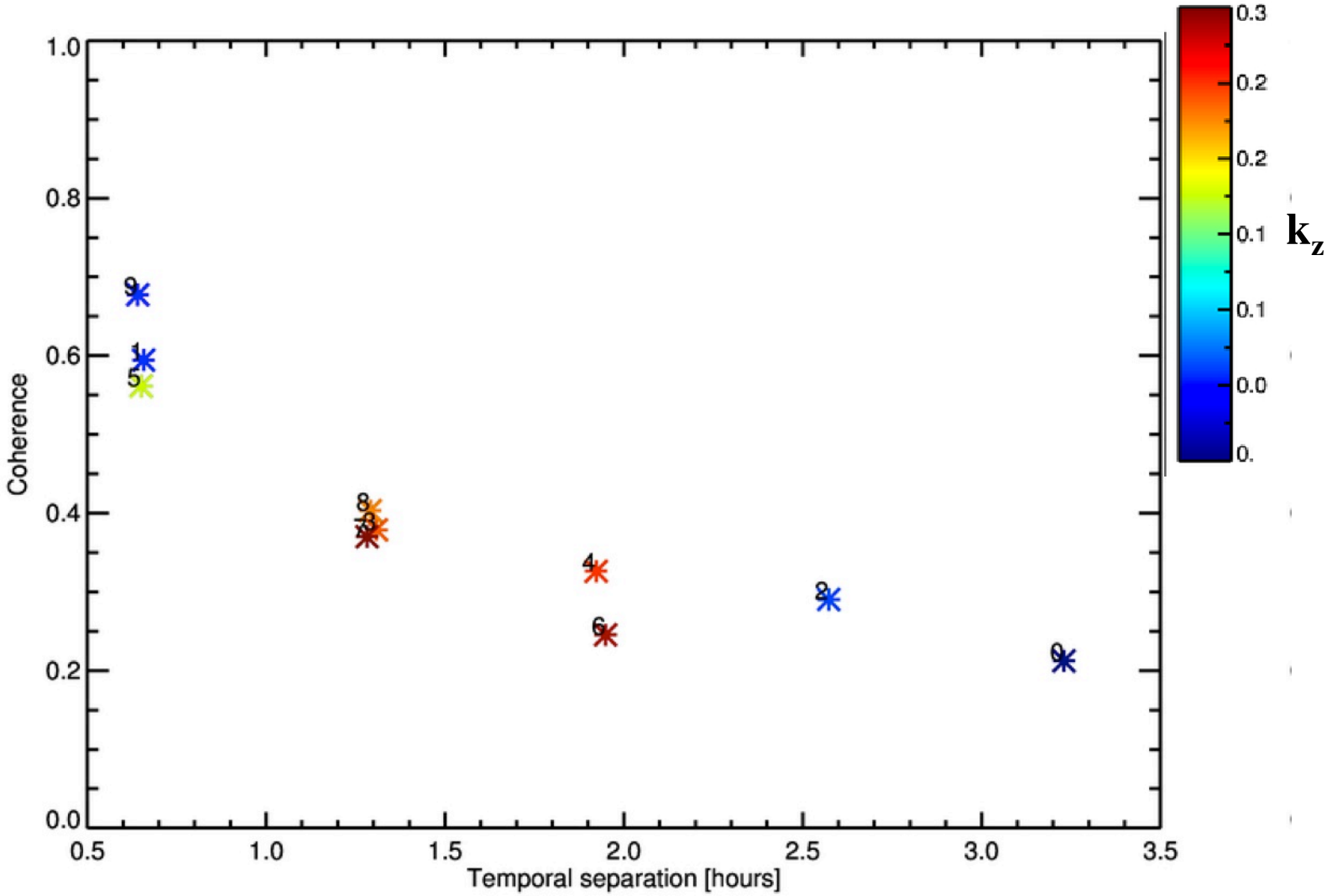

JPL

Area II

Average Backscatter and Correlation Images

- Average backscatter for all passes and average correlation over all interferometric pairs.

$\sigma_{hh} + \sigma_{vv}$ $\sigma_{hh} - \sigma_{vv}$ σ_{hv}

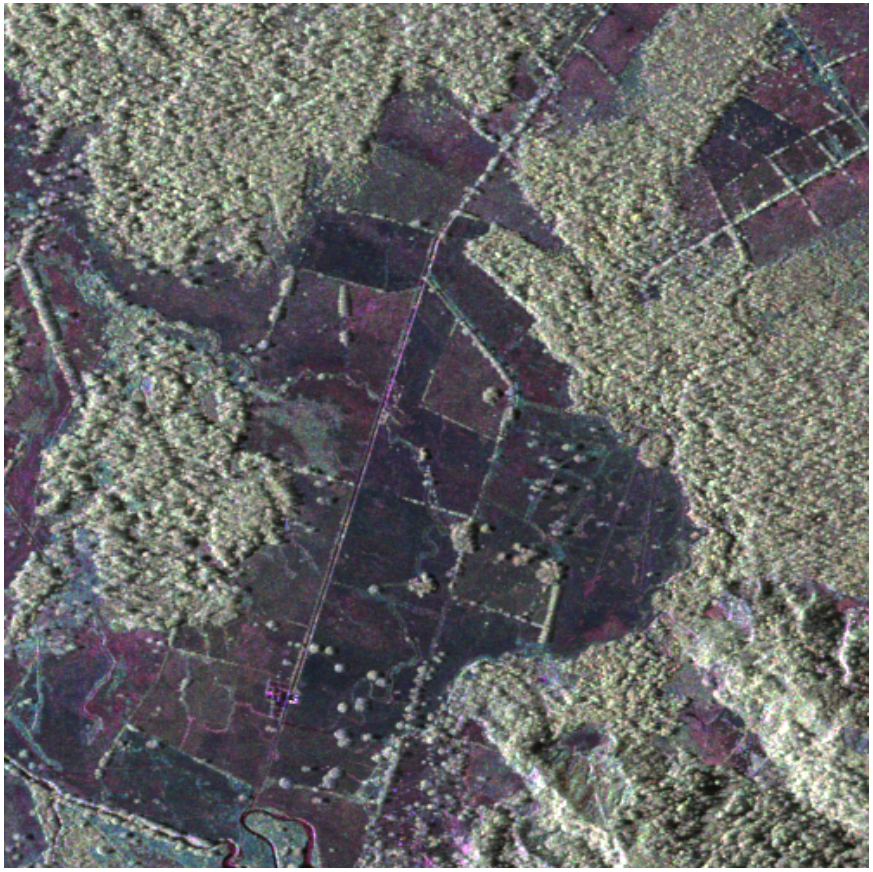

γ_{hh+vv} γ_{hh-vv} γ_{hv}

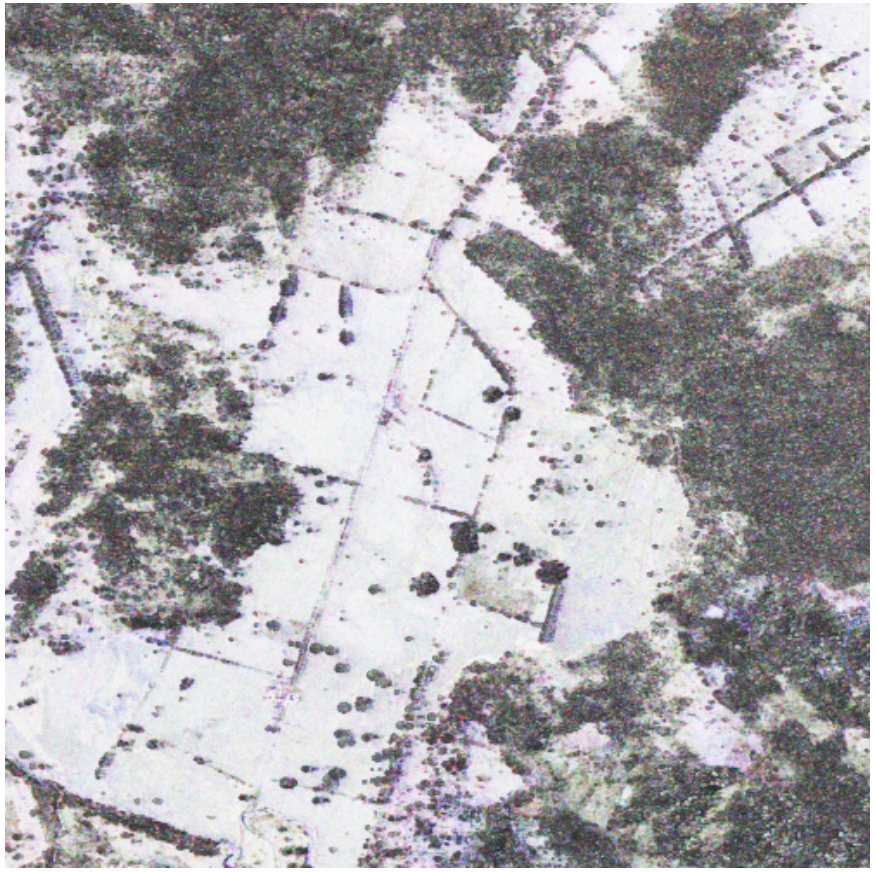

k_z and Ambiguity Heights for Site II

- k_z and ambiguity heights for the interferometric passes.

k_z

Track #	1	2	3	4	5
1		0.006	0.041	0.173	0.218
2			0.046	0.178	0.224
3				0.132	0.178
4					0.046
5					

Ambiguity Height

Track #	1	2	3	4	5
1		1139	155	36	29
2			136	35	28
3				48	35
4					137
5					

Note that for baselines 4, 5, 7, 8 that the ambiguity is smaller than the ICESAT vegetation height estimates.

Correlation, Phase Image Matrix

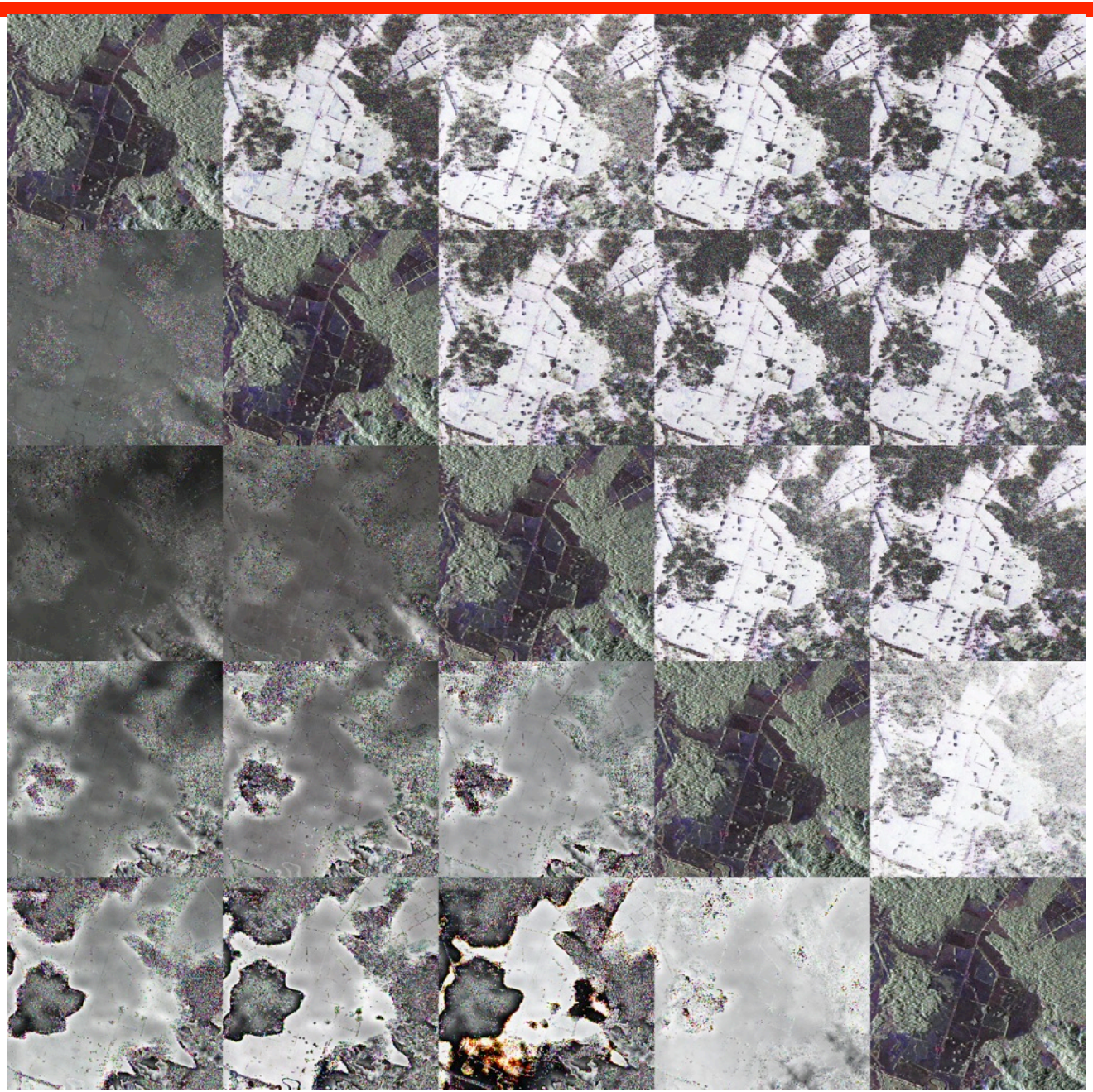

PolinSAR Vegetation Height Estimates

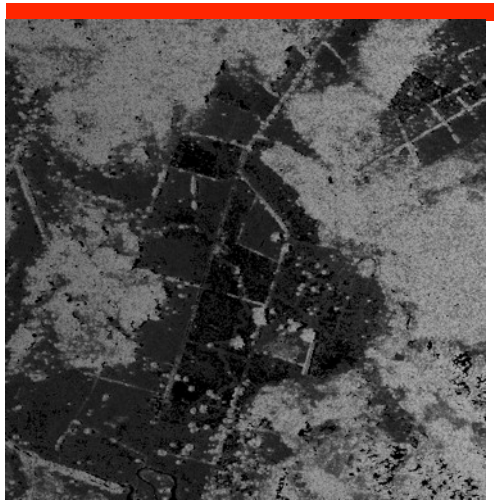

Baseline #: 3
B: 79 m
Δt: 1.3 h

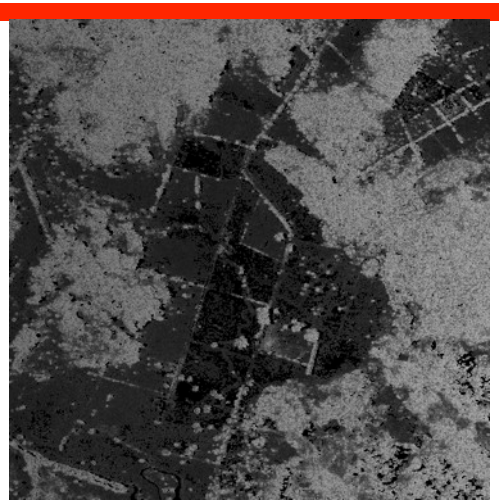

Baseline #: 4
B: 79 m
Δt: 1.9 h

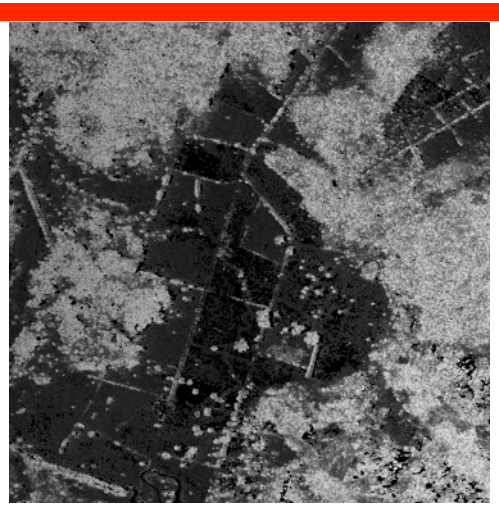

Baseline #: 5
B: 60 m
Δt: 0.7 h

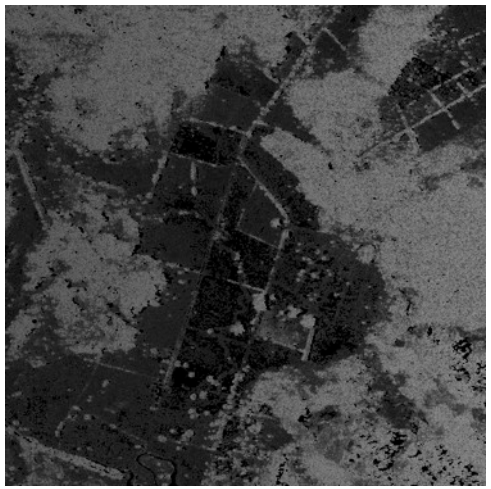

Baseline #: 6
B: 99 m
Δt: 1.9 h

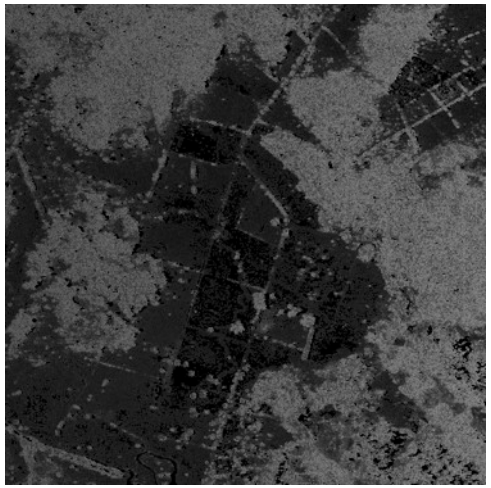

Baseline #: 7
B: 99 m
Δt: 1.3 h

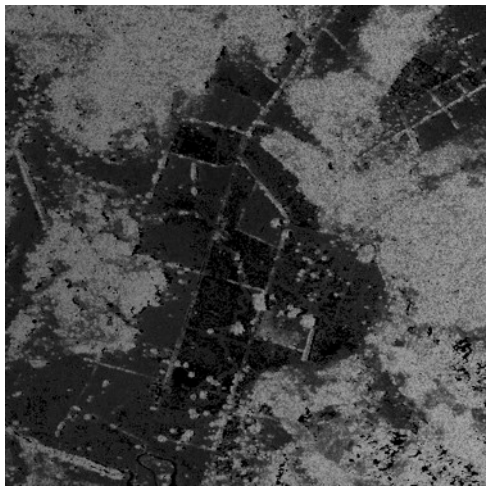

Baseline #: 8
B: 81 m
Δt: 1.3 h

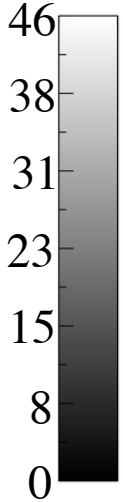

Average Height and Histograms

- Height estimate averaged over all interferometric pairs and height histograms for the various baselines.

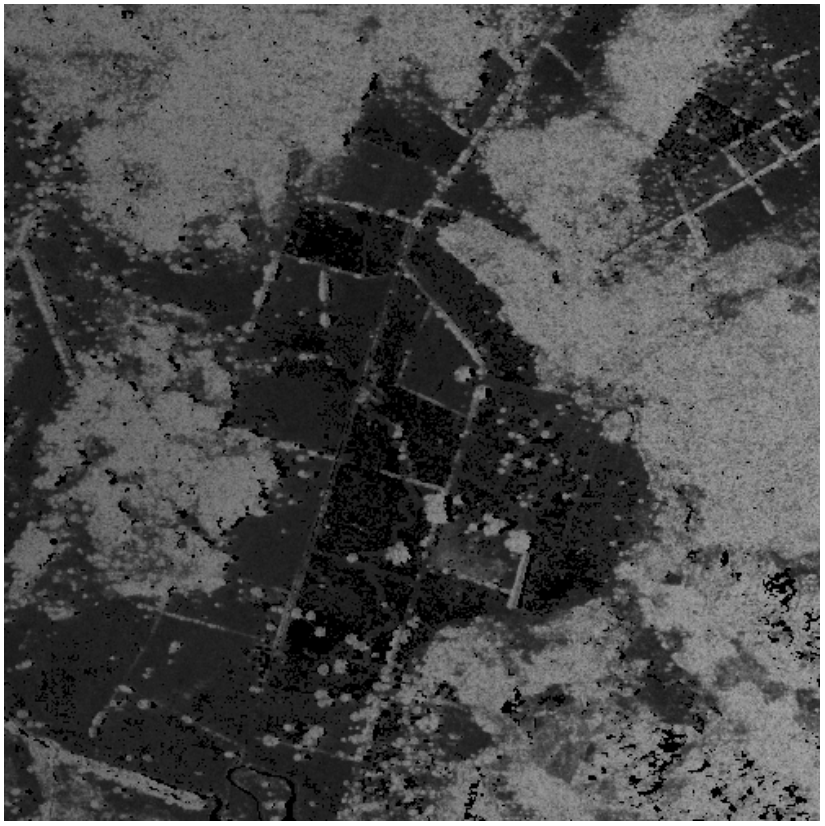

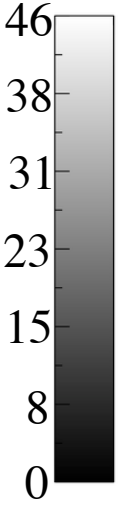

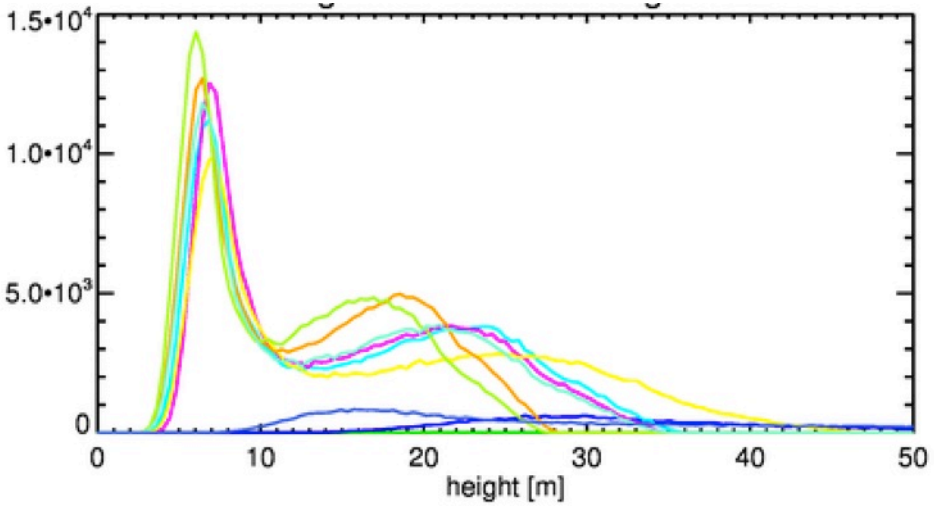

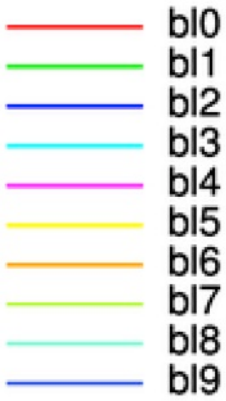

JPL

Area III

Average Backscatter and Correlation Images

$\sigma_{hh} + \sigma_{vv}$ $\sigma_{hh} - \sigma_{vv}$ σ_{hv}

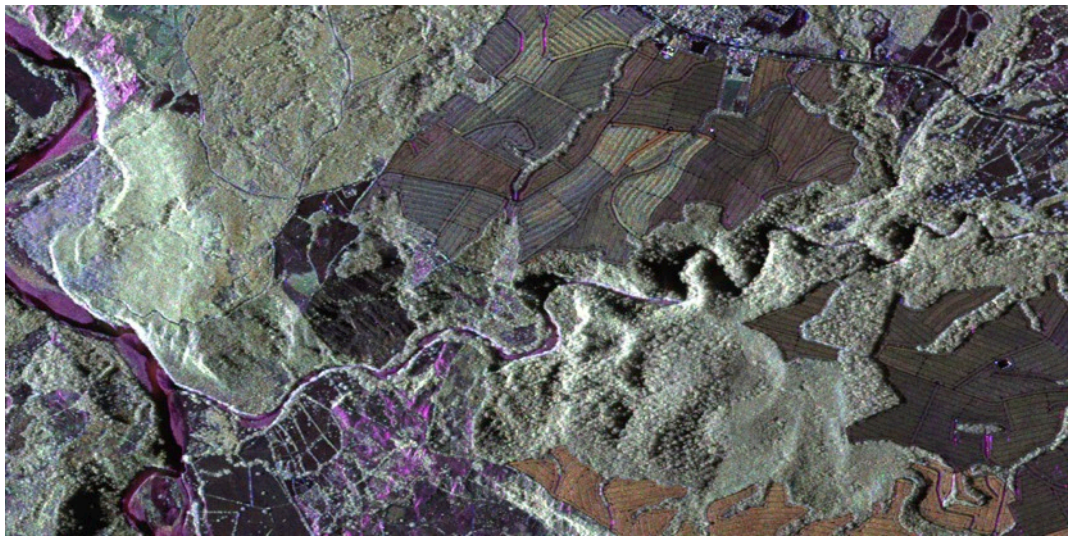

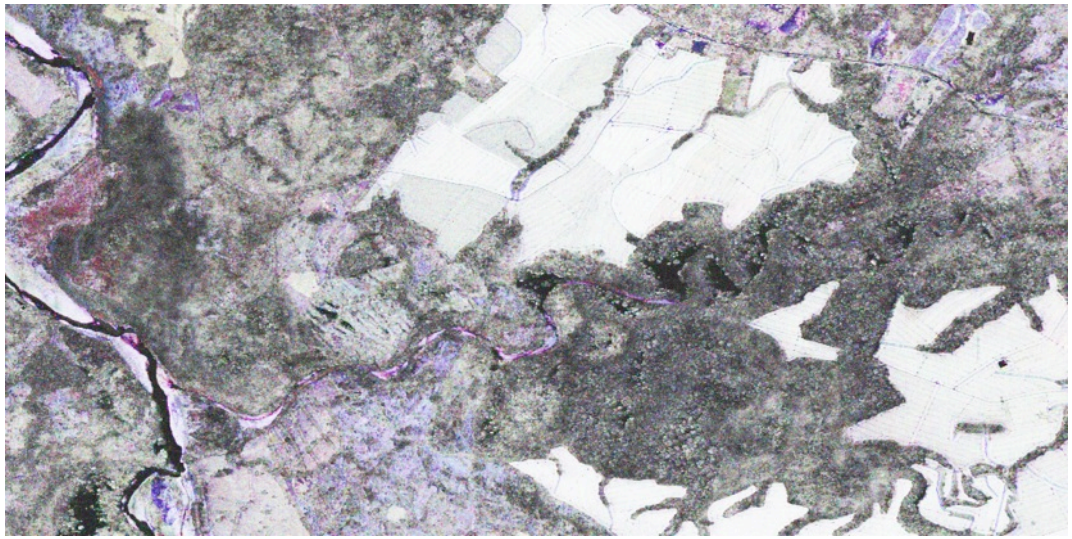

γ_{hh+vv} γ_{hh-vv} γ_{hv}

- Average backscatter for all passes and average correlation over all interferometric pairs.

k_z and Ambiguity Heights for Site III

- k_z and ambiguity heights for the interferometric passes.

k_z

Track #	1	2	3	4	5
1		0.001	0.030	0.128	0.163
2			0.031	0.129	0.164
3				0.098	0.133
4					0.035
5					

Ambiguity Height

Track #	1	2	3	4	5
1		5090	211	49	39
2			204	48	38
3				64	47
4					180
5					

Note that for baselines 6,7 that the ambiguity height is very close the maximal lidar tree heights.

Correlation, Phase Image Matrix

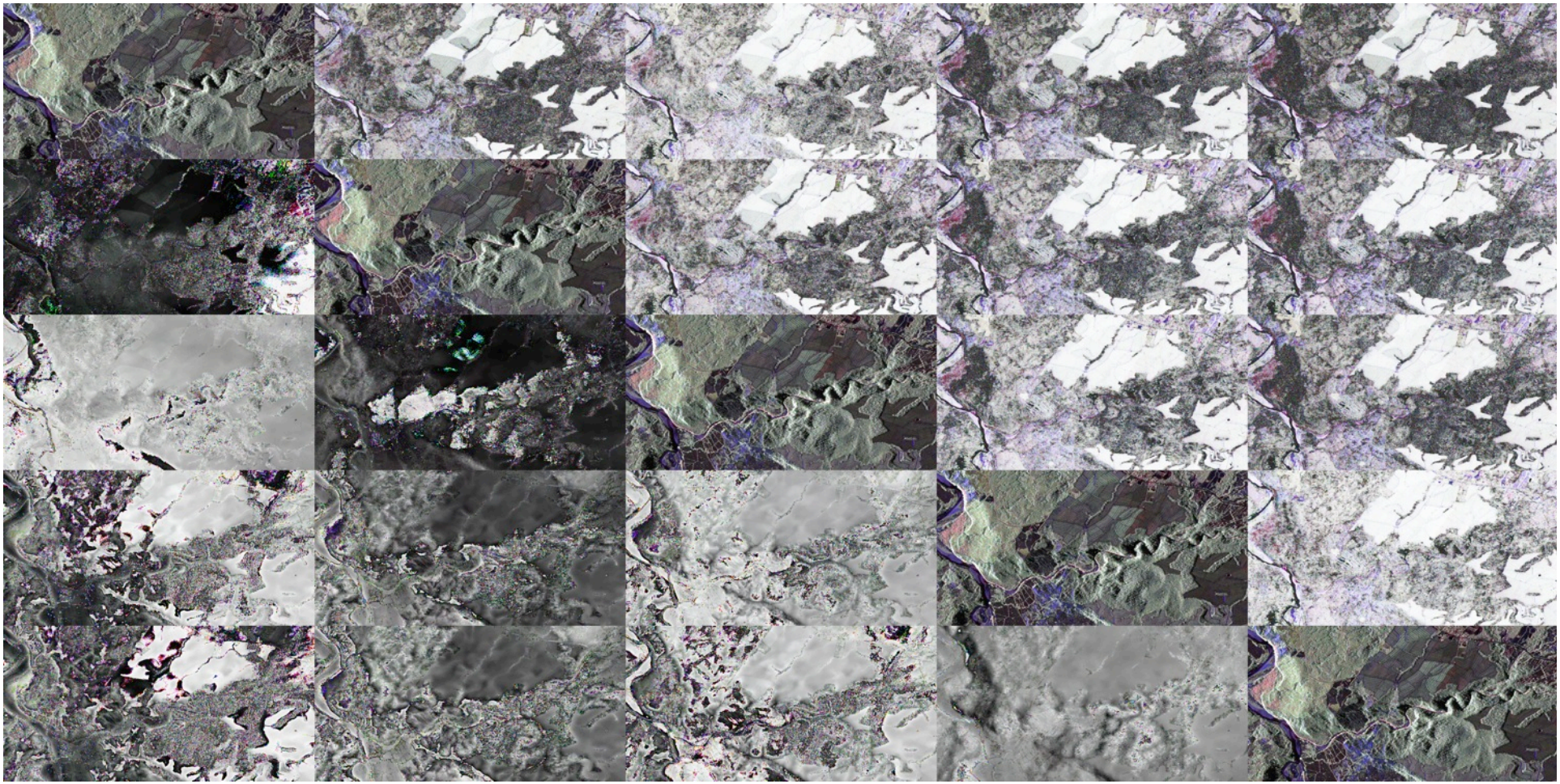

PolinSAR Vegetation Height Estimates

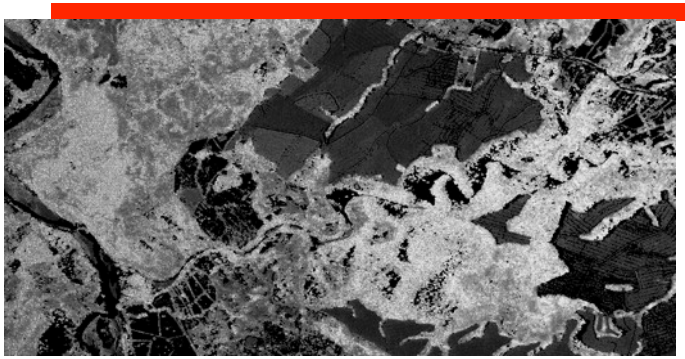

Baseline #: 3
B: 79 m
Δt: 1.3 h

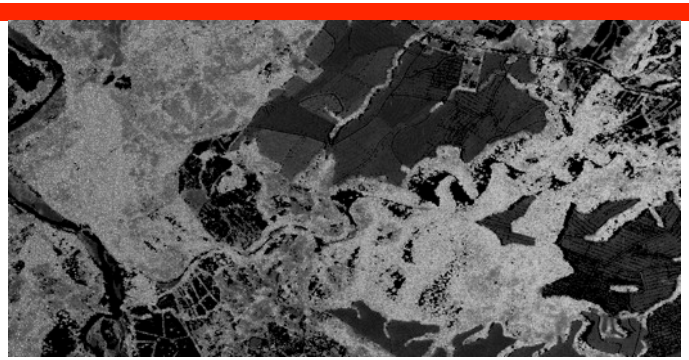

Baseline #: 6
B: 99 m
Δt: 1.9 h

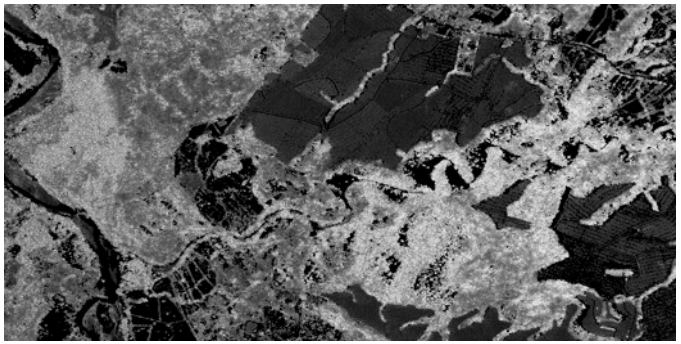

Baseline #: 4
B: 79 m
Δt: 1.9 h

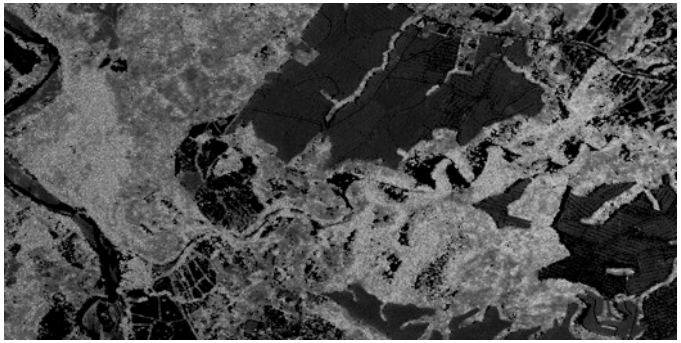

Baseline #: 7
B: 99 m
Δt: 1.3 h

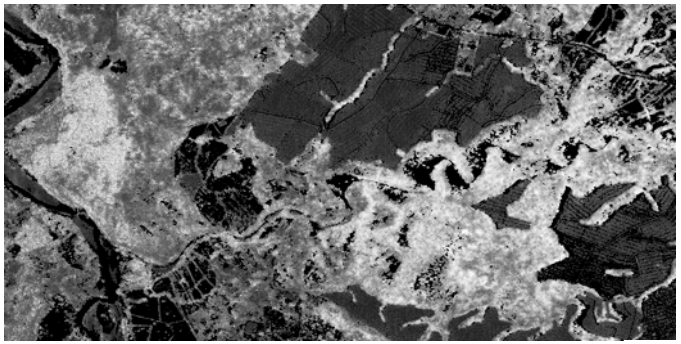

Baseline #: 5
B: 60 m
Δt: 0.7 h

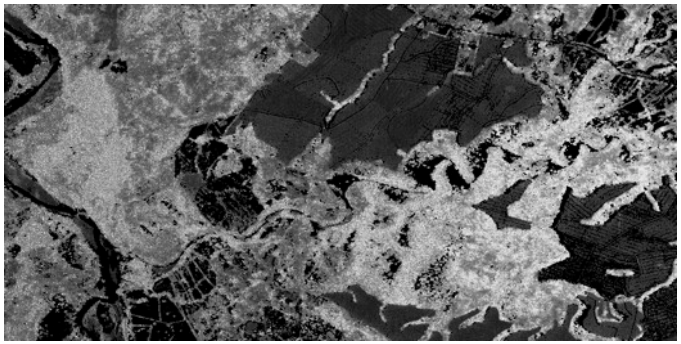

Baseline #: 8
B: 81 m
Δt: 1.3 h

0 8 15 23 31 38 46

Average Height and Histograms

- Height estimate averaged over all interferometric pairs and height histograms for the various baselines.

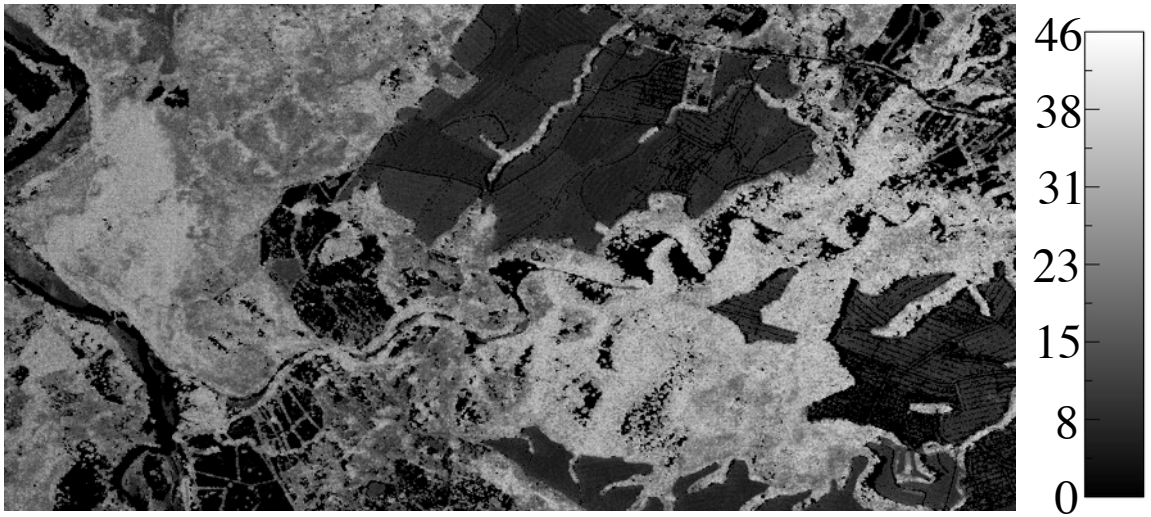

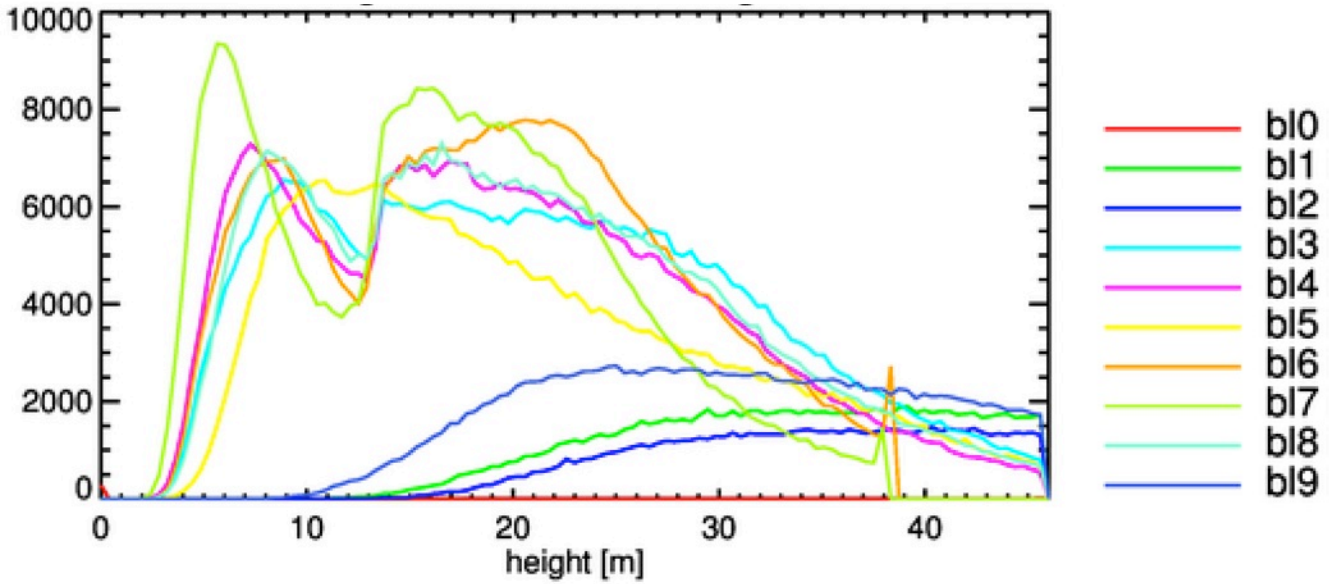

JPL

Area VII

Average Backscatter and Correlation Images

- Average backscatter for all passes and average correlation over all interferometric pairs.

$\sigma_{hh} + \sigma_{vv}$ $\sigma_{hh} - \sigma_{vv}$ σ_{hv} γ_{hh+vv} γ_{hh-vv} γ_{hv}

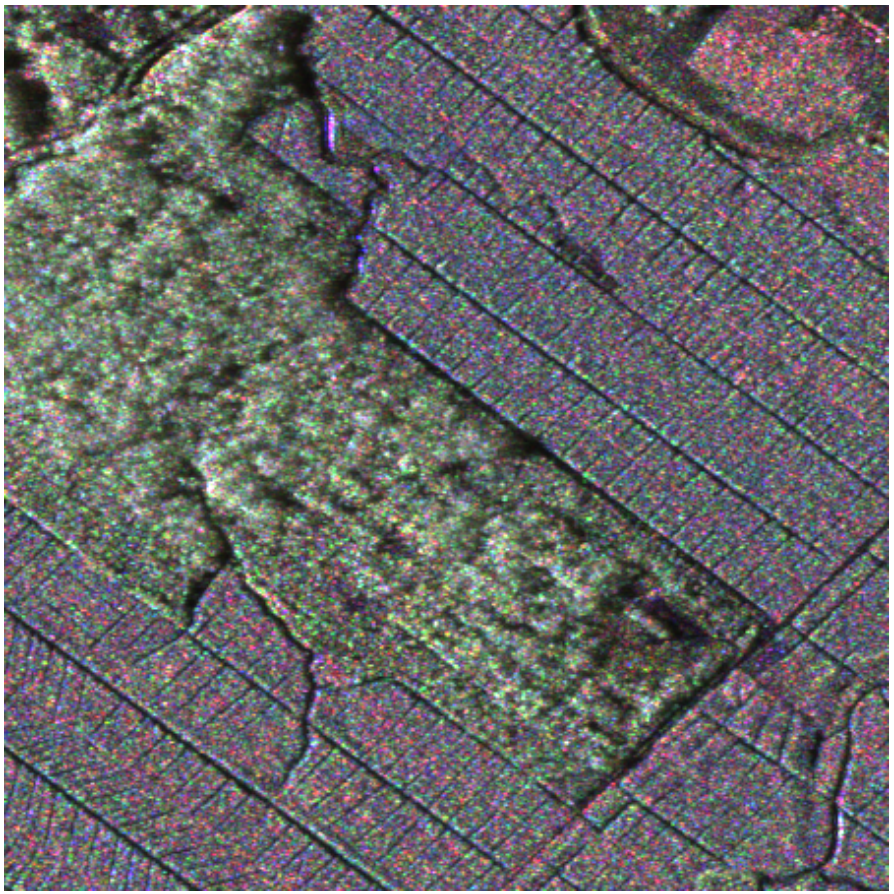

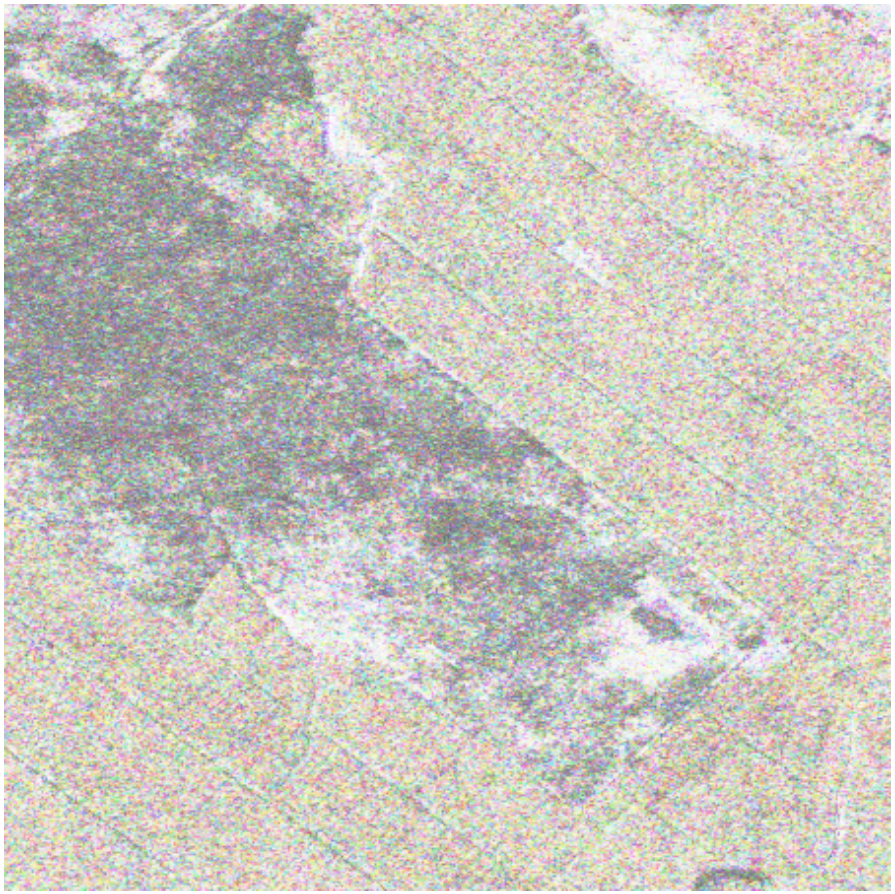

k_z and Ambiguity Heights for Site VI

- k_z and ambiguity heights for the interferometric passes.

k_z

Track #	1	2	3	4	5
1		0.004	0.027	0.115	0.140
2			0.031	0.120	0.145
3				0.088	0.113
4					0.025
5					

Ambiguity Height

Track #	1	2	3	4	5
1		1443	233	54	44
2			200	52	43
3				71	55
4					251
5					

Correlation, Phase Image Matrix

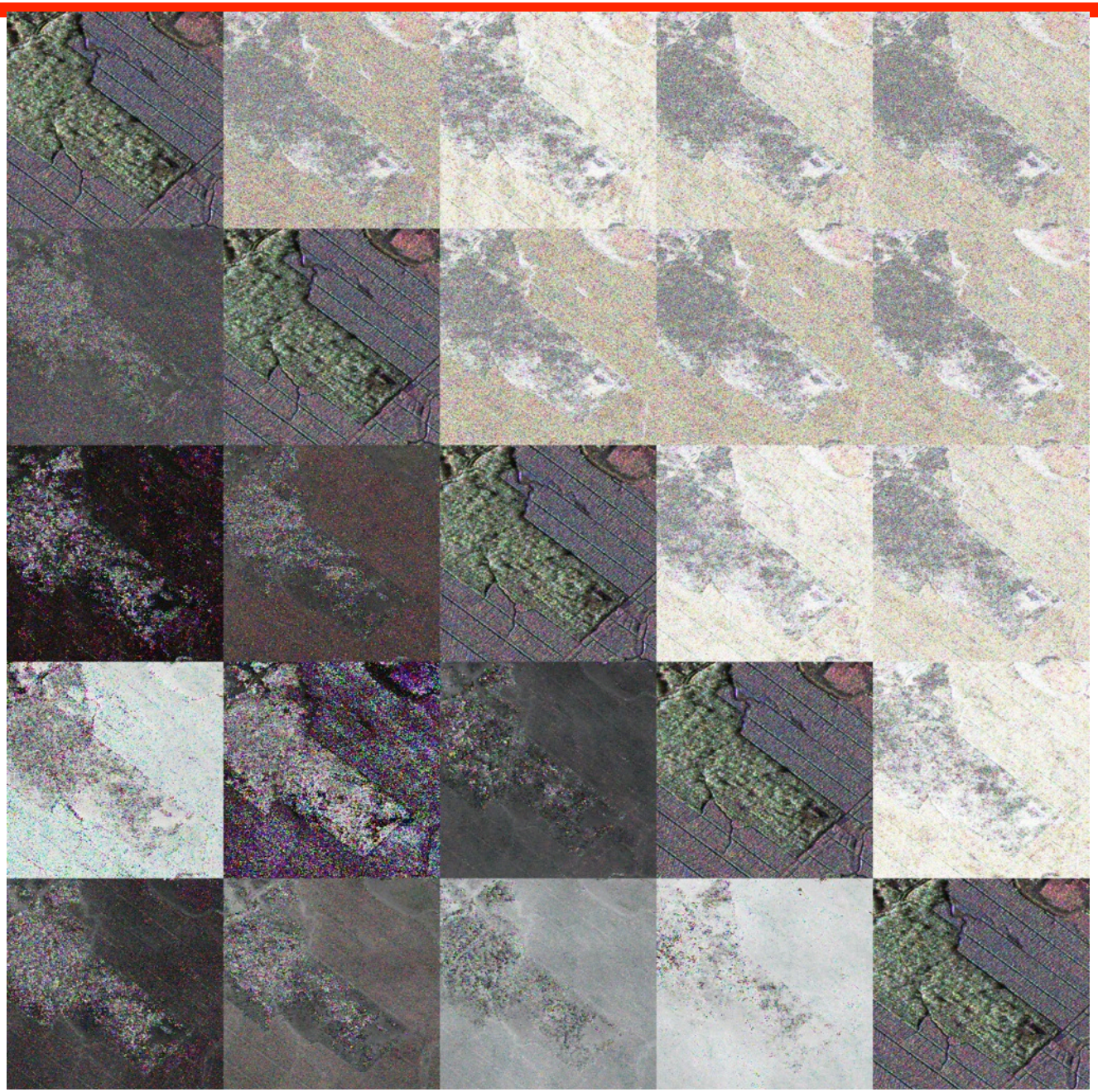

PolinSAR Vegetation Height Estimates

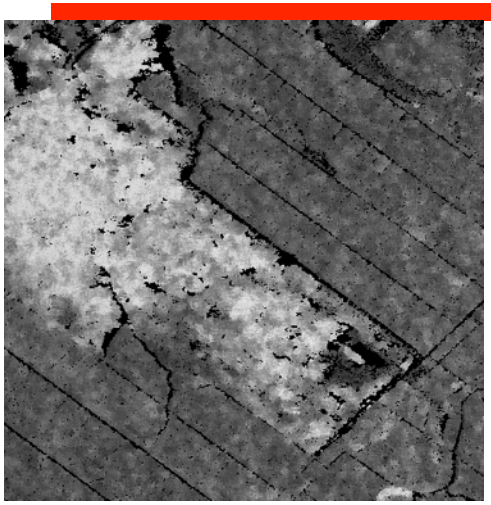

Baseline #: 3
B: 79 m
Δt: 1.3 h

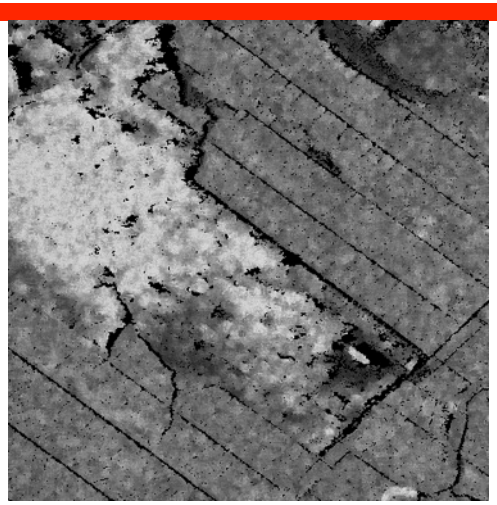

Baseline #: 4
B: 79 m
Δt: 1.9 h

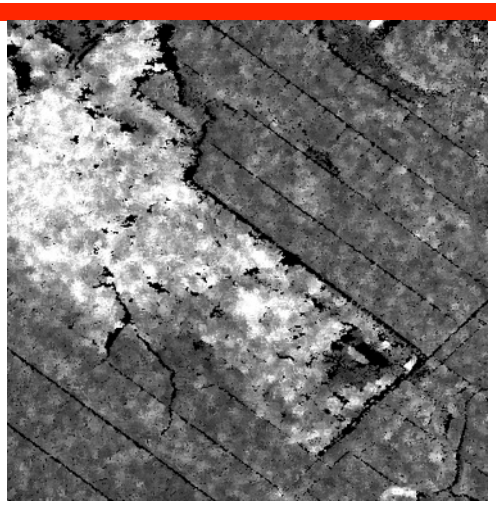

Baseline #: 5
B: 60 m
Δt: 0.7 h

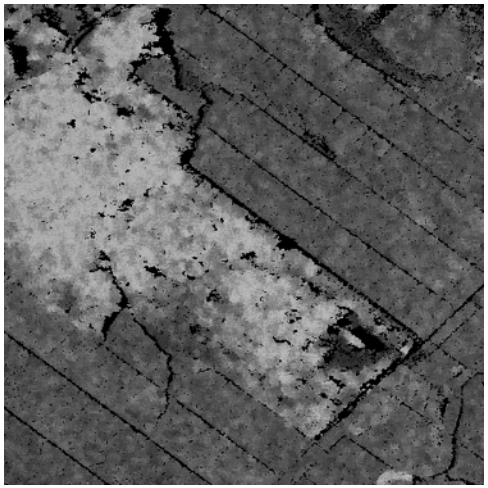

Baseline #: 6
B: 99 m
Δt: 1.9 h

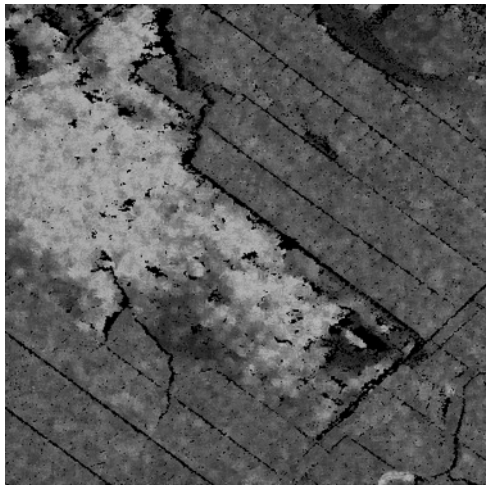

Baseline #: 7
B: 99 m
Δt: 1.3 h

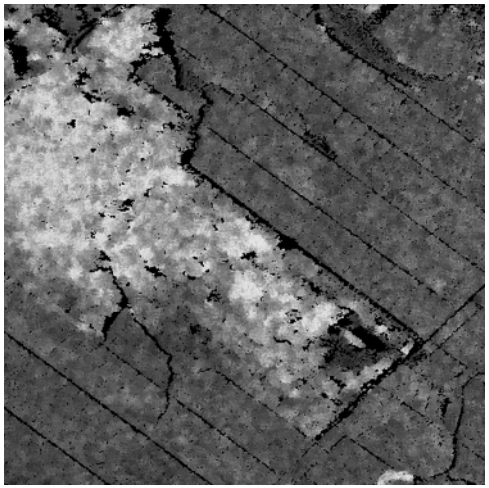

Baseline #: 8
B: 81 m
Δt: 1.3 h

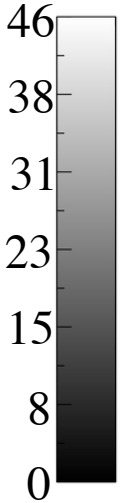

Average Height and Histograms

- Height estimate averaged over all interferometric pairs and height histograms for the various baselines.

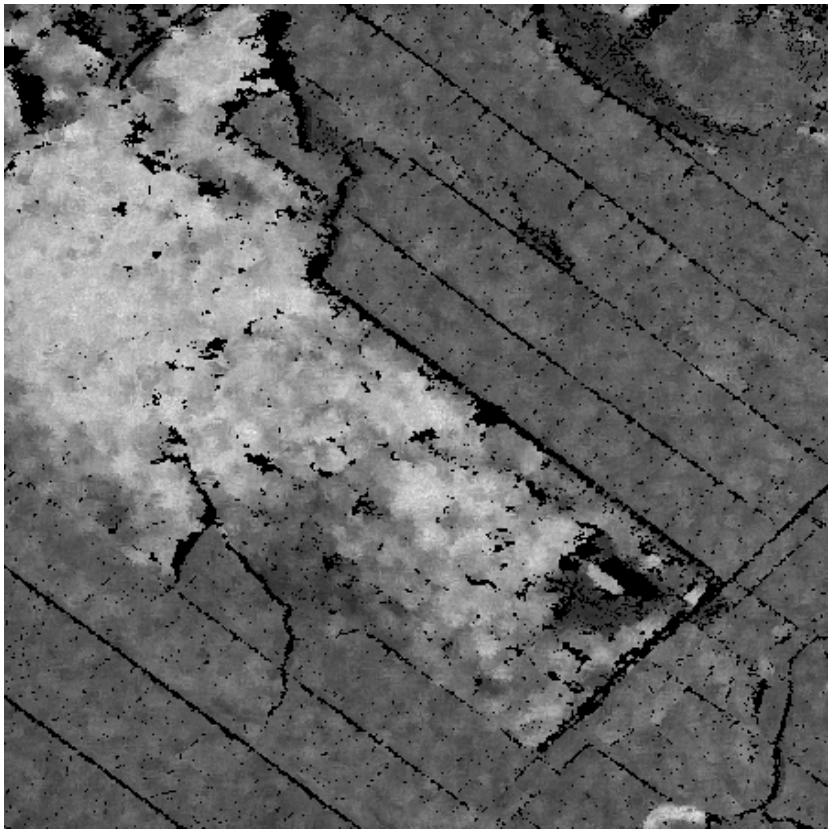

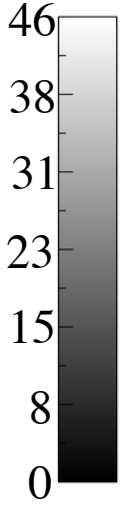

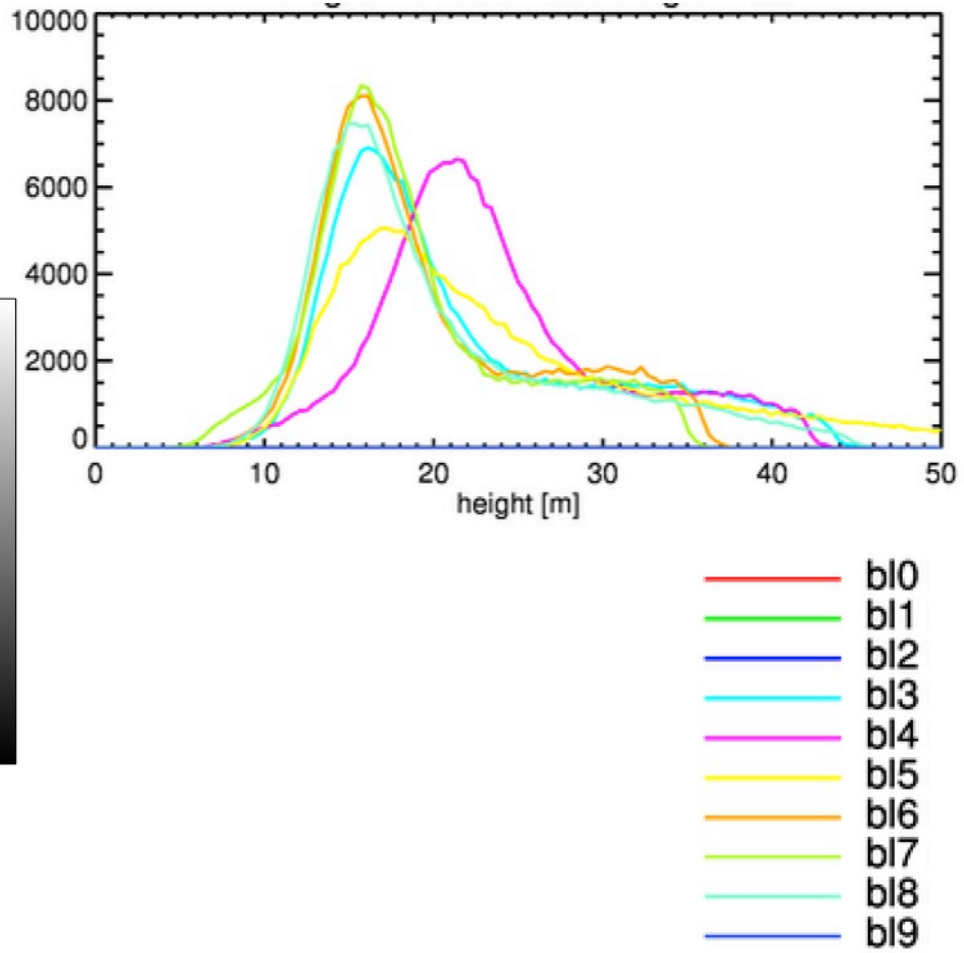

Conclusions

- UAVSAR imaged La Amistad with multiple physical and temporal baselines at La Amistad national park.
- Temporal decorrelation, even for temporal baselines in the range of a few hours, impacted the PolinSAR inversions at La Amistad.
- Need greater baseline diversity to get good k_z diversity for all incidence angles for the range of vegetation heights in this area. Larger baselines have ambiguity heights smaller the larger tree height and smallest baselines do not have enough sensitivity.
- Shapes of histogram of tree height for the different baselines look fairly similar in most cases, however they are shifted and scaled, most likely due to temporal decorrelation.
  - When the baselines are small, we observe higher inverted heights because the decorrelation inverted heights scale with a larger height ambiguity.

Questions?